Molecular Cell
Article

Star-PAP Control of BIK Expression and Apoptosis Is Regulated by Nuclear PIPKIα and PKCδ Signaling

Weimin Li,[1,4] Rakesh S. Laishram,[1,4] Zhe Ji,[3] Christy A. Barlow,[1,5] Bin Tian,[3] and Richard A. Anderson[1,2,*]
[1]Department of Pharmacology
[2]Molecular and Cellular Pharmacology Program
School of Medicine and Public Health, University of Wisconsin–Madison, Madison, WI 53706, USA
[3]Department of Biochemistry and Molecular Biology, New Jersey Medical School, University of Medicine and Dentistry of New Jersey, Newark, NJ 07103, USA
[4]These authors contributed equally to this work
[5]Present address: Chem Risk, LLC, 4840 Pearl East Circle, Suite 300 West, Boulder, CO 80301, USA
*Correspondence: raanders@wisc.edu
DOI 10.1016/j.molcel.2011.11.017

SUMMARY

BIK protein is an initiator of mitochondrial apoptosis, and *BIK* expression is induced by proapoptotic signals, including DNA damage. Here, we demonstrate that 3′ end processing and expression of *BIK* mRNA are controlled by the nuclear PI4,5P_2-regulated poly(A) polymerase Star-PAP downstream of DNA damage. Nuclear PKCδ is a key mediator of apoptosis, and DNA damage stimulates PKCδ association with the Star-PAP complex where PKCδ is required for Star-PAP-dependent *BIK* expression. PKCδ binds the PI4,5P_2-generating enzyme PIPKIα, which is essential for PKCδ interaction with the Star-PAP complex, and PKCδ activity is directly stimulated by PI4,5P_2. Features in the *BIK* 3′ UTR uniquely define Star-PAP specificity and may block canonical PAP activity toward *BIK* mRNA. This reveals a nuclear phosphoinositide signaling nexus where PIPKIα, PI4,5P_2, and PKCδ regulate Star-PAP control of *BIK* expression and induction of apoptosis. This pathway is distinct from the Star-PAP-mediated oxidative stress pathway indicating signal-specific regulation of mRNA 3′ end processing.

INTRODUCTION

BCL2-interacting killer (BIK) protein activates the mitochondrial apoptotic pathway by inducing Ca^{2+} release from the endoplasmic reticulum (ER) and the remodeling of the mitochondrial cristae that releases cytochrome c and activates caspase 9 (Chinnadurai et al., 2008; Germain et al., 2002). BIK is a tumor suppressor, a prognostic marker, and a therapeutic target for cancers, and *BIK* expression is induced by DNA damage, viral infection, and cytokines (Chinnadurai et al., 2008). BIK expression inhibits antiapoptotic effects of oncoproteins and viral infection and induces cell apoptosis (Han et al., 1996). In contrast, loss of *BIK* per se fails to alter apoptotic profile in hematopoietic and endothelial cells, while combined deficiency of BIK and BIM (another BH3-only protein) exhibits additive effect on apoptosis in germ cells (Coultas et al., 2005), indicating a critical yet redundant role of BIK. The cellular levels of BIK are controlled by both posttranslational and transcriptional mechanisms (Hur et al., 2006; Marshansky et al., 2001). However, these regulatory mechanisms for BIK expression and the signaling pathways mediating these steps are not well defined.

Protein kinase C (PKC) isoforms are key regulators of apoptosis (Brodie and Blumberg, 2003; Reyland, 2007) and PKCδ, a novel PKC subfamily member, is required for apoptosis in response to several stimuli (Brodie and Blumberg, 2003), including DNA damage (Yoshida, 2007). Mice deficient in PKCδ are resistant to γ-irradiation-induced apoptosis (Humphries et al., 2006). DNA damage-induced p53 activation and protein levels are similar in primary cells derived from $PKC\delta^{+/+}$ and $PKC\delta^{-/-}$ mice, indicating that PKCδ functions downstream of the DNA damage response (Humphries et al., 2006). PKCδ regulates the mitochondrial apoptosis pathway (Humphries et al., 2006; Steinberg, 2004) and this requires nuclear targeting of PKCδ (Yoshida, 2007).

PKCδ is targeted to different cellular compartments, depending on its phosphorylation status (Rybin et al., 2004). Phosphorylation of tyrosines 64 and 187 on PKCδ appears important for PKCδ's role in apoptosis induced by DNA damage (Blass et al., 2002). However, tyrosine phosphorylation only serves to amplify the later stages of the apoptosis signal and is not required for the nuclear targeting of full-length PKCδ (Blass et al., 2002). After initiation of apoptosis, PKCδ is cleaved by caspase or other proteases into regulatory and catalytic domains, and these further activate downstream signaling cascades (DeVries et al., 2002). The cleaved catalytic fragment of PKCδ is important for the progression of apoptosis (Ghayur et al., 1996), and the regulatory fragment is required for the optimal function of PKCδ (Blass et al., 2002).

Activated PKCδ could also induce apoptosis without being proteolytically cleaved by caspase (Tanaka et al., 2003). It was proposed that the catalytic fragment and the full-length PKCδ target different nuclear substrates at different stages of apoptosis (Steinberg, 2004). There are substrates for nuclear PKCδ activity, but it is not clear which of these are critical for induction of apoptosis. PKC isoforms are regulated by

phosphoinositide signaling through generation of diacylglycerol by cleavage of phosphatidylinositol-4,5-bisphosphate (PI4,5P_2), and some PKCs directly interact with and are regulated by PI4,5P_2 (Chauhan and Brockerhoff, 1988; Huang and Huang, 1991; Lee and Bell, 1991). The role of phosphoinositides in the modulation of nuclear PKCδ is not defined.

In nuclei, there is a distinct phosphatidylinositol cycle that is independent of the cytosolic pathway (Barlow et al., 2010; Cocco et al., 1987). Nuclear diacylglycerol kinase theta (DGK-θ), phospholipase C beta 1 (PLCβ1), PI4,5P_2, and phosphatidylinositol-4-phosphate 5-kinase I alpha (PIPKIα) all were detected and targeted to nuclear speckles (Gonzales and Anderson, 2006; Tabellini et al., 2003). These findings suggest a mechanism where nuclear signals emanating from PI4,5P_2 may regulate nuclear localized PKC isoforms.

Recently gene expression has been shown to be directly regulated by nuclear phosphoinositide signaling through a noncanonical poly(A) polymerase, *s*peckle-*t*argeted PIPKIα-*r*egulated *p*oly(*A*) *p*olymerase (Star-PAP) (Mellman et al., 2008). Star-PAP controls the expression of a subset of genes by assembling into a distinct 3′ end cleavage and polyadenylation complex on its target mRNAs. Star-PAP associates with regulatory proteins such as PIPKIα and casein kinase I (CKI) isoforms α and ε, which are required for 3′ end processing (Gonzales et al., 2008; Laishram et al., 2011; Mellman et al., 2008). PI4,5P_2 directly and specifically controls the activity of Star-PAP (Mellman et al., 2008). Star-PAP has been proposed to function as a signal-regulated effector of mRNA 3′ end processing that may integrate into different pathways (Barlow et al., 2010). In this study, we identified *BIK* as a direct target of Star-PAP and defined a Star-PAP-specific binding region on the *BIK* mRNA. Upon DNA damage signaling, Star-PAP, PKCδ, and PIPKIα form a functional complex required for *BIK* expression in response to the apoptotic signal induced by etoposide. These data define Star-PAP as a molecular target for nuclear PKCδ that controls the expression of BIK, an important switch in the mitochondrial apoptosis pathway.

RESULTS

Star-PAP and Associated PIPKIα Are Required for *BIK* Expression

Cellular BIK is increased in response to DNA damage signaling (Fu et al., 2007). Gene microarray analysis of Star-PAP knockdown cells implicated *BIK* as a Star-PAP target (Mellman et al., 2008). To determine the role of Star-PAP in BIK expression, the mRNA and the protein levels of BIK were analyzed in the absence or presence of etoposide treatment. Etoposide (VP-16) is a DNA-damaging compound that inhibits topoisomerase II and induces apoptosis (Baldwin and Osheroff, 2005). The optimal time used for etoposide treatment was determined by time-course experiments. In the DNA fragmentation analysis, DNA condensation was initiated at 4 hr post etoposide treatment (Figure S1A). Concomitantly, BIK protein levels were substantially increased during this time (Figure S1B). Therefore, this time after etoposide treatment was chosen for most of the experiments, except for the DNA laddering and the caspase 3/7 activity assays as described below.

Star-PAP control of *BIK* expression was measured by quantitative RT-PCR after Star-PAP knockdown by RNA interference (RNAi). *BIK* mRNA level decreased 8-fold after Star-PAP knockdown, proportional to the efficiency of Star-PAP knockdown (Figure 1A). The etoposide-potentiated *BIK* expression was reduced to the same extent (Figure 1A). Similarly, when PIPKIα was knocked down, both the basal and the etoposide-induced *BIK* expression were decreased (Figures 1A and S1D). Remarkably, while etoposide enhanced the cellular BIK protein content, knockdown of Star-PAP or PIPKIα diminished the BIK protein greater than 15-fold in both etoposide treated and nontreated cells (Figures 1A and S1D). Simultaneous knockdown of both Star-PAP and PIPKIα did not significantly enhance the block of *BIK* mRNA or protein expression (Figure 1A), indicating that Star-PAP and PIPKIα act in the same pathway for BIK expression.

Since Star-PAP is a poly(A) polymerase, we investigated the 3′ end processing and polyadenylation of *BIK* pre-mRNA using 3′ RACE assays with cDNA synthesized from total RNA isolated from cells after RNAi knockdown of Star-PAP or PIPKIα and etoposide treatment. Distinct RACE products for *BIK* were observed with the control cell mRNAs and an increase was noted after stimulation with etoposide (Figures 1B and S1D). There was a loss of RACE products upon Star-PAP or PIPKIα knockdown regardless of etoposide treatment (Figures 1B and S1D). Ectopic re-expression of the wild-type (wt) but not the polymerase dead (pd) *Star-PAP* or the kinase dead (kd) *PIPKIα*, with silencing mutations (sm) that are resistant to the RNAi, rescued the loss of *BIK* in Star-PAP or PIPKIα knockdown cells (Figures 1B and S1D). The changes in BIK protein levels followed the similar pattern (Figures 1B and S1D). The Star-PAP nontarget mRNA, *glyceraldehyde 3-phosphate dehydrogenase* (*GAPDH*), was not affected by knockdown of Star-PAP/PIPKIα nor by stimulation with etoposide (Figures 1B and S1D). These data demonstrate that the Star-PAP poly(A) polymerase activity and the ability of PIPKIα to generate PIP_2 are required for BIK expression.

Consistent with the Star-PAP role in the cleavage of its target *HO-1* pre-mRNA (Laishram and Anderson, 2010; Mellman et al., 2008), Star-PAP or PIPKIα knockdown resulted in an accumulation of uncleaved *BIK* pre-mRNA (Figures 1B and S1D). However, DNA damage stimulation reduced the uncleaved *BIK* message compared to the unstimulated control (Figures 1B and S1D). Expression of *Star-PAP*$^{wt/sm}$ and *Star-PAP*$^{pd/sm}$ rescued the knockdown-induced cleavage defect (Figure 1B), indicating that Star-PAP protein but not its activity is required for 3′ end cleavage. In contrast, re-expression of *PIPKIα*$^{wt/sm}$ but not *PIPKIα*$^{kd/sm}$ alleviated the cleavage defect resembling the rescue of the *BIK* mRNA 3′ end formation in the RACE assays. This indicates a role for the PIPKIα kinase activity, PIP_2 production, in the regulation of Star-PAP processivity toward *BIK*. These data collectively demonstrate that Star-PAP controls both the 3′ end cleavage and polyadenylation of the *BIK* mRNA downstream of DNA damage.

PKCδ Associates with and Directly Phosphorylates Star-PAP

To identify signaling molecules that transmit apoptotic/DNA damage signals to Star-PAP-mediated *BIK* expression, we

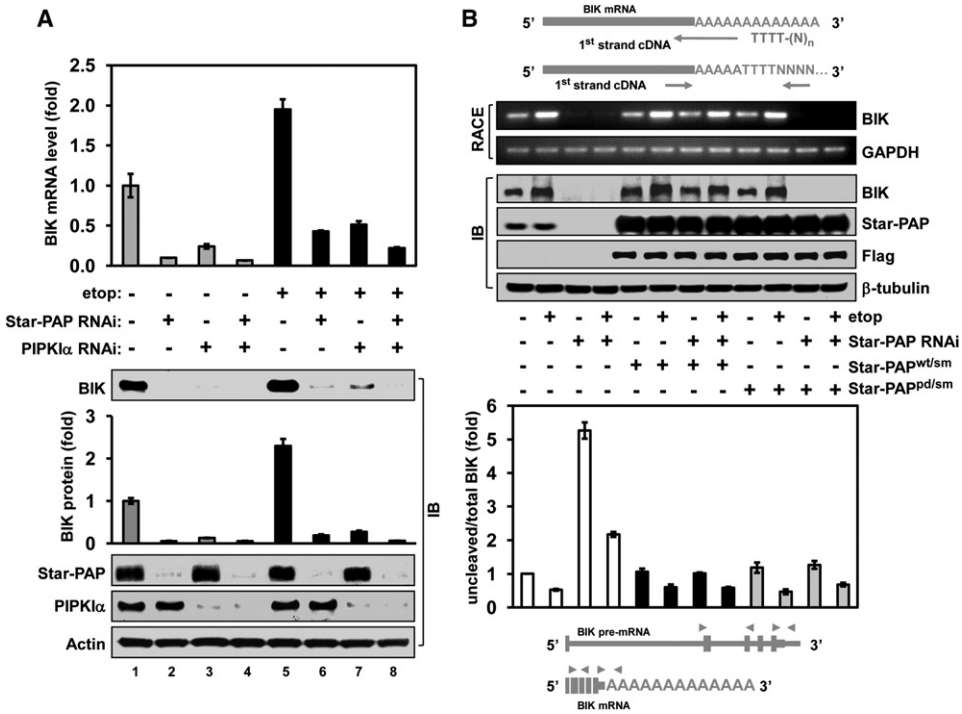

Figure 1. BIK Expression Is Controlled by Star-PAP and PIPKIα

(A) *BIK* mRNA levels (upper panel) in cells with or without Star-PAP or/and PIPKIα RNAi knockdown in presence or absence of etoposide (100 μM, 4 hr) were analyzed by quantitative RT-PCR. mRNA expression was normalized to the mock-treated control. Error bars represent standard error of the mean (SEM) of three independent experiments in triplicate for each experimental condition. BIK protein levels (lower panels) under the same experimental conditions were measured by IB and densitometrically quantified.

(B) Star-PAP controls *BIK* mRNA 3′ end processing. The level of the *BIK* mRNA poly(A) tail message compared to that of the control *GAPDH* under the same assay conditions was analyzed by 3′ RACE. The top panel illustrates the 3′ end of *BIK* mRNA with poly(A) tail and the location of the gene-specific and the 3′ adapter primers (short arrows). The effect of Star-PAP knockdown on the cleavage of the *BIK* mRNA was investigated by quantitative RT-PCR. The bottom panel shows the *BIK* mRNA and the location of the primer sets (arrow heads) used for the detection of cleavage. Error bars represent SEM of three independent experiments with triplicate for each experimental condition. See also Figure S1.

investigated protein kinase activities associated with Star-PAP. When affinity-purified Star-PAP complex was treated with phorbol 12-myristate 13-acetate (PMA), associated protein kinase activity toward Star-PAP was stimulated (Figure 2A). PMA activates a number of kinases, including PKC isoforms (Brose and Rosenmund, 2002). Therefore the association of members of the PKC family with Star-PAP was analyzed by immunoblotting (IB). This identified PKCδ but not PKCα (Figure 2B) or any other PKC isoforms (data not shown) in the affinity purified Star-PAP complex under these conditions. The association of PKCδ with Star-PAP was further confirmed by immunoprecipitation (IP) and IB of endogenous Star-PAP and PKCδ (Figure 2C). However, the GST-tagged PKCδ failed to pull down the His-tagged Star-PAP in vitro, indicating that the association of PKCδ with Star-PAP is indirect (data not shown).

Star-PAP and the associated PIPKIα are spatially targeted to nuclear speckles in the cells (Mellman et al., 2008). Our data demonstrate that PKCδ was also targeted to foci that partially colocalized with Star-PAP (Figure 2D, first four panels) and with the speckle marker SC-35 (Figure 2D, middle and last four panels) as shown by immunofluorescence microscopy (IF). Since PKCδ is a component of the Star-PAP complex and may phosphorylate Star-PAP, the effect of exogenous PKCδ kinase activity toward Star-PAP was analyzed. Recombinant PKCδ phosphorylated the purified Star-PAP complex in a dose-dependent fashion, and PMA treatment further enhanced PKCδ-dependent phosphorylation of Star-PAP (Figure 2E). Consistently, PKCδ phosphorylated the recombinant His-tagged Star-PAP (Figure 2F), indicating that Star-PAP is a direct substrate of PKCδ. In both cases, IP of Star-PAP under denaturing conditions demonstrated that the 120 kDa ^{32}P-phosphorylated band was indeed Star-PAP (Figures 2E and 2F, lower panels).

PKCδ Directly Interacts with PIPKIα, and PI4,5P$_2$ Stimulated PKCδ Kinase Activity toward Star-PAP

PIPKIα and PKCδ are components of Star-PAP complex. It is reported that some PKC isoforms interact with and are regulated by PI4,5P$_2$ (Chauhan and Brockerhoff, 1988; Huang and Huang, 1991; Lee and Bell, 1991). We hypothesized that PI4,5P$_2$ could be a direct regulator of PKCδ. As PIP kinases often define PI4,5P$_2$ signaling specificity by interacting with PI4,5P$_2$ effectors (Heck et al., 2007), the interaction between

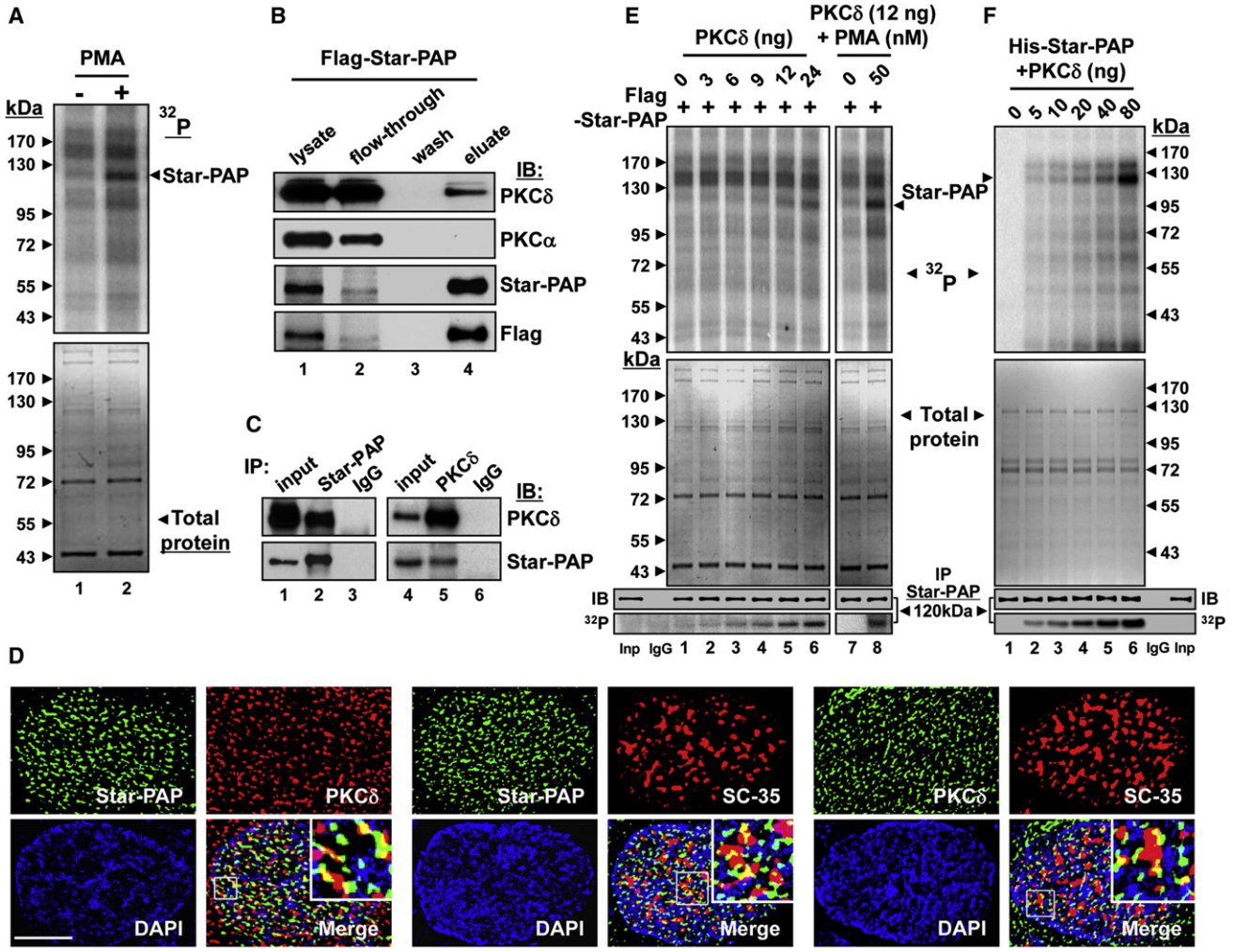

Figure 2. PKCδ Associates with Star-PAP in the Nucleus and Directly Phosphorylates Star-PAP

(A) Affinity purified FLAG-tagged Star-PAP complex contains PMA-stimulated kinase activities. Coomassie staining of the SDS-PAGE gel showed total protein loading.

(B) PKCδ was detected in the FLAG-Star-PAP complex by IB.

(C) PKCδ was coIPed with endogenous Star-PAP and was confirmed by reverse IP.

(D) PKCδ colocalized with Star-PAP in the nucleus and targeted to nuclear speckles as shown by IF. The boxed areas were magnified and shown as insets. Scale bar = 10 μm.

(E) Purified recombinant PKCδ dose-dependently phosphorylated the Star-PAP complex, and the phosphorylation was further stimulated by PMA.

(F) The recombinant PKCδ directly phosphorylated His-tagged Star-PAP. In addition to protein staining, the Star-PAP protein in the reactions was examined by IP/IB using Star-PAP antibody, and the ^{32}P-phosphorylated Star-PAP was identified by phosphorimaging after IP (E and F bottom panels).

PIPKIα and PKCδ was investigated by in vitro GST pull-down assays. This demonstrated direct binding of PIPKIα to PKCδ (Figure 3A). Moreover, endogenous PKCδ was coimmunoprecipitated with PIPKIα and vice versa (Figure 3B), indicating that PKCδ and PIPKIα associate in vivo. To determine if PKCδ activity is regulated by PI4,5P$_2$, PKCδ kinase activity was assayed using myelin basic protein (MBP) as generic PKCδ substrate in the presence of an increasing amount of PI4,5P$_2$. PI4,5P$_2$ stimulated PKCδ kinase activity toward MBP (Figure 3C). Most importantly, PI4,5P$_2$ stimulated PKCδ activity toward Star-PAP purified from cell lysates (Figure 3D).

PIPKIα Is Required for DNA Damage-Stimulated Interaction of PKCδ and Star-PAP

PKCδ translocates into the nucleus in response to DNA damage, and this nuclear translocation is required for the initiation of apoptosis (DeVries et al., 2002). As Star-PAP controls *BIK* expression and interacts with PKCδ in the nucleus, the impact of the apoptotic signal on PKCδ association with Star-PAP was assessed by reciprocal IP/IB of Star-PAP and PKCδ after DNA damage. PKCδ protein levels increased and peaked at 4 to 8 hr post etoposide treatment (Figure S1B), and the association of PKCδ with Star-PAP was concurrently enhanced (Figures 4A

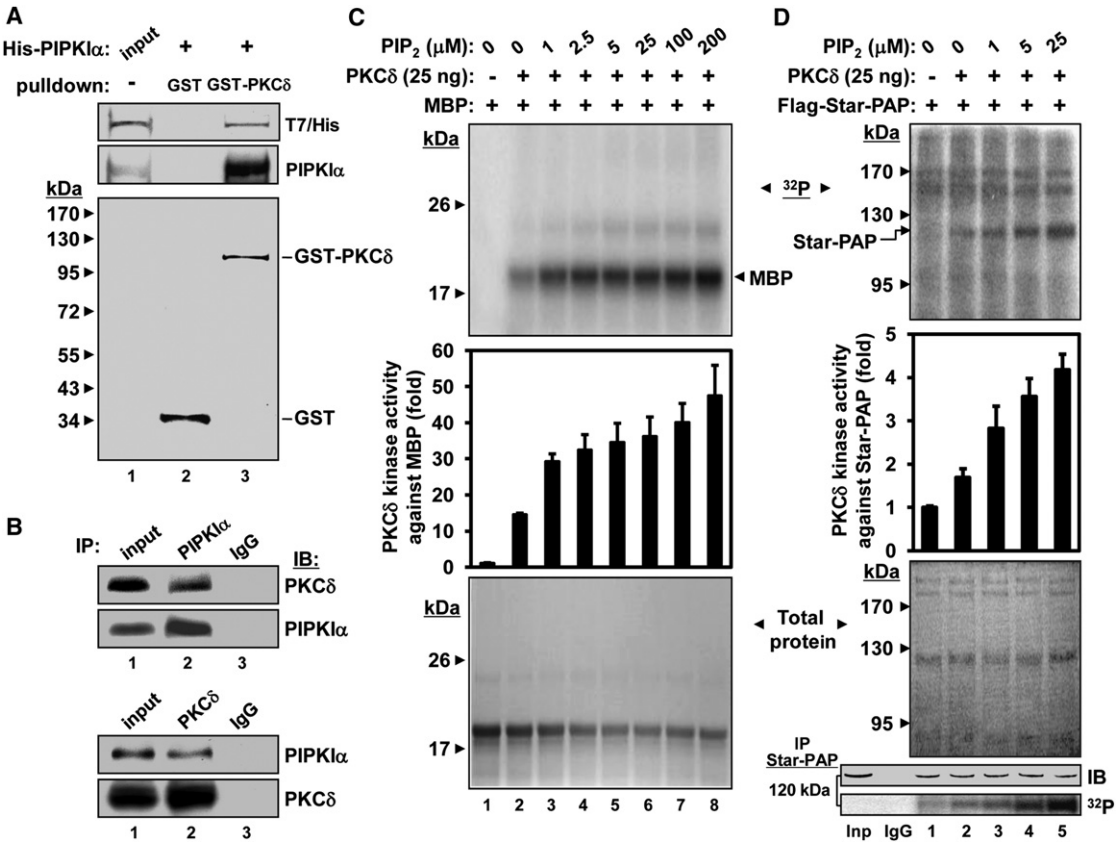

Figure 3. PKCδ Directly Interacts with PIPKIα, and PI4,5P$_2$ Stimulates PKCδ Kinase Activity

(A) GST pull-down assay revealed direct interaction of PKCδ and PIPKIα.

(B) Endogenous PKCδ coIPed with PIPKIα.

(C) PI4,5P$_2$ dose-dependently increased PKCδ kinase activity toward MBP.

(D) PI4,5P$_2$ augmented PKCδ phosphorylation of the affinity purified Star-PAP. The phosphorimages were quantified. Error bars represent standard deviation of three independent experiments (middle panels of C and D). Total proteins in the gels were stained with Coomassie blue. Star-PAP contents and specific phosphorylation in the reactions were evaluated by IP followed by phosphorimaging and IB (D bottom panels).

and S1C). The increased PKCδ interaction with Star-PAP was supported by IF staining, which demonstrated that PKCδ increased its nuclear speckle colocalization with SC-35 by 1.5 fold and with Star-PAP by 2.3 fold after etoposide treatment (Figure S2A).

PIPKIα and PKCδ directly interact and are integrated into the Star-PAP complex, and DNA damage enhances PKCδ association with Star-PAP. Thus, it is plausible that PIPKIα and the locally produced PI4,5P$_2$ may modulate PKCδ activity and assembly into the Star-PAP complex. To determine the impact of PIPKIα on the interaction of PKCδ with Star-PAP, PIPKIα was knocked down and the cells were treated with or without etoposide. PIPKIα knockdown diminished the association of PKCδ with Star-PAP (Figures 4B and 4C), confirming that PIPKIα is required for the interaction of PKCδ with the Star-PAP complex. However, DNA damage had no detectable impact on the association of PIPKIα with Star-PAP (Figures S2B and S2C). In addition, PKCδ knockdown did not alter the association of Star-PAP with PIPKIα in both etoposide-treated and non-treated cells (Figures S2D and S2E). Star-PAP is incorporated into the transcriptional complex, and the association of RNA Pol II with the Star-PAP complex was also impaired after PIPKIα and PKCδ knockdown (Figures 4B, 4C, S2D, and S2E), indicating that the interaction of the Star-PAP complex with the transcription machinery requires PIPKIα and PKCδ.

These data demonstrate that PIPKIα within the Star-PAP complex is required for the recruitment of and serves as a docking site for PKCδ in vivo. This suggests that PIPKIα could be a substrate for PKCδ or may directly modulate its activity. Recombinant PKCδ failed to phosphorylate PIPKIα in vitro (data not shown). To determine if PIPKIα directly regulates PKCδ activity, increasing PIPKIα was combined with PKCδ, and kinase activity toward MBP or Star-PAP was assayed. Remarkably, PIPKIα inhibited PKCδ activity toward Star-PAP (Figure S3A) and MBP (data not shown) in a dose-dependent fashion. The PIPKIα inhibition of PKCδ activity was relieved by addition of PI4,5P$_2$ (Figures 4D and S3B), again indicating that PIPKIα activity and PI4,5P$_2$ production modulate PKCδ activity. Surprisingly, PMA failed to stimulate PKCδ activity toward recombinant Star-PAP when PKCδ was associated with PIPKIα (Figure S3C).

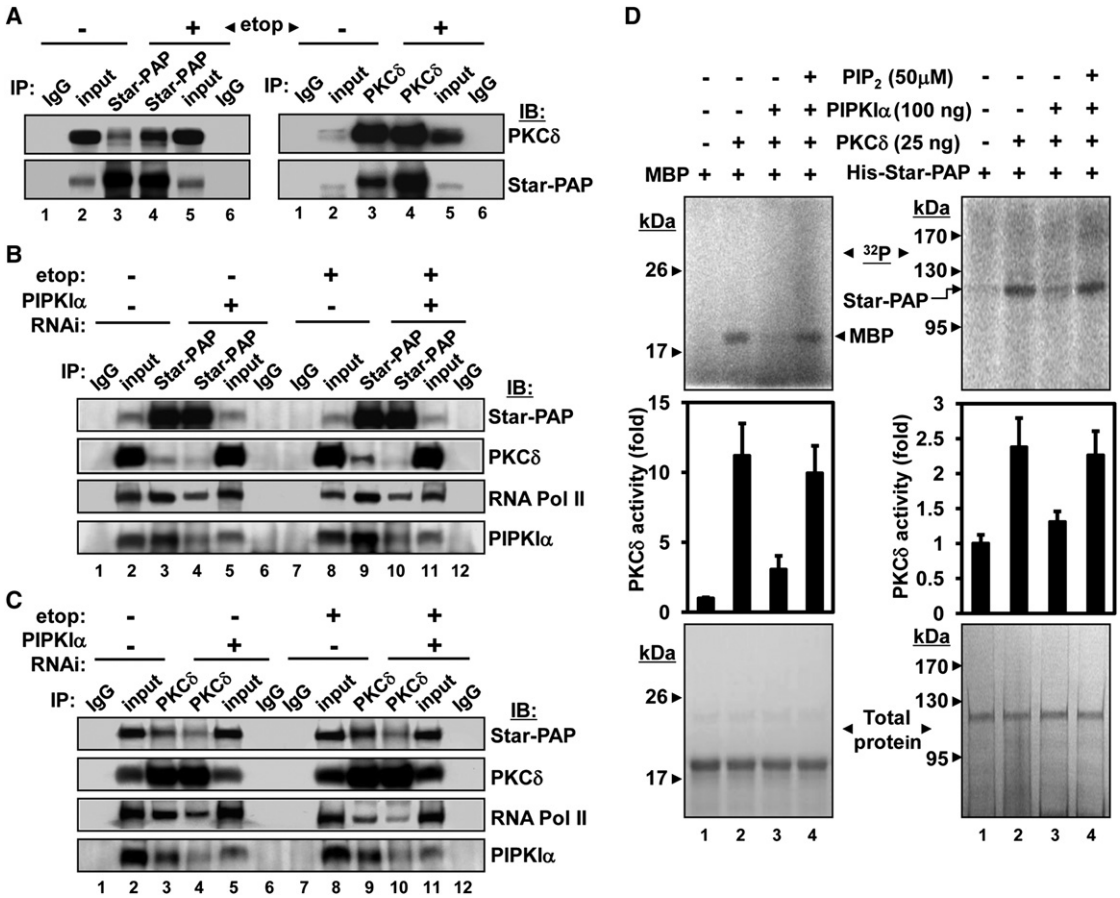

Figure 4. PIPKIα Is Required for DNA Damage-Stimulated PKCδ and Star-PAP Interaction

(A) Etoposide increased the association between PKCδ and Star-PAP, as analyzed by IP and IB.

(B and C) Knockdown of PIPKIα attenuated the association of Star-PAP, PKCδ, and RNA Pol II as examined by IP of Star-PAP (B) or PKCδ (C) and IB for the respective proteins.

(D) PIPKIα inhibited PKCδ phosphorylation of MBP and His-Star-PAP, which was relieved by PI4,5P$_2$. The phosphorimages were quantified (middle panels). Error bars represent standard deviation of three independent experiments. See also Figures S1, S2, and S3.

This supports the idea that PI4,5P$_2$ is the primary lipid messenger for PKCδ activation in this signaling pathway.

PKCδ Regulates Star-PAP Activity, *BIK* Expression, and Is Associated with *BIK* mRNA

BIK and PKCδ both mediate the mitochondrial apoptosis pathway (Germain et al., 2002; Humphries et al., 2006). As Star-PAP controls *BIK* expression and the association of PKCδ with Star-PAP is increased in response to DNA damage, the possibility that PKCδ modulates *BIK* expression was explored. Knockdown of PKCδ dramatically reduced both basal and etoposide-stimulated *BIK* mRNA and protein levels (Figure 5A), equivalently to Star-PAP and PIPKIα knockdown. Re-expression of the wild-type (wt) but not the kinase dead (kd) *PKCδ* rescued the endogenous PKCδ knockdown phenotype of *BIK* mRNA and protein loss (Figure 5A). The expression of kinase dead *PKCδ* appeared to act as a dominant negative mutant, which blocked BIK expression (Figure 5A). This indicates that the interaction and kinase activity of PKCδ are required for the regulation of Star-PAP.

As PKCδ interacts with and phosphorylates Star-PAP, the role of PKCδ in the 3′ end processing of *BIK* mRNA was investigated by using 3′ RACE assays. Knockdown of PKCδ resulted in a loss of RACE product in control and DNA-damaged cells (Figure 5A), similarly to the knockdown of Star-PAP and PIPKIα (Figures 1B and S1D). This phenotype was rescued by the expression of $PKC\delta^{wt/sm}$ but not $PKC\delta^{kd/sm}$ (Figure 5A). Expression of $PKC\delta^{kd/sm}$ also decreased the RACE product similarly to PKCδ knockdown (Figure 5A). The control *GAPDH* was not affected by knockdown or ectopic expression of *PKCδ* or DNA damage (Figure 5A). However, knockdown of PKCδ had no effect on the cleavage of *BIK* pre-mRNA in control cells, but increased the uncleaved message upon DNA damage (Figure S4A). While $PKC\delta^{wt/sm}$ overexpression rescued the cleavage defect, $PKC\delta^{kd/sm}$ failed to restore *BIK* pre-mRNA cleavage (Figure S4A). These data demonstrate that PKCδ is required for the generation of mature *BIK* mRNA in vivo. Consistent with this role in *BIK* mRNA 3′ end processing, PKCδ and PIPKIα associate with the *BIK* UTR RNA along with Star-PAP, as shown by RNA immunoprecipitation (RIP)

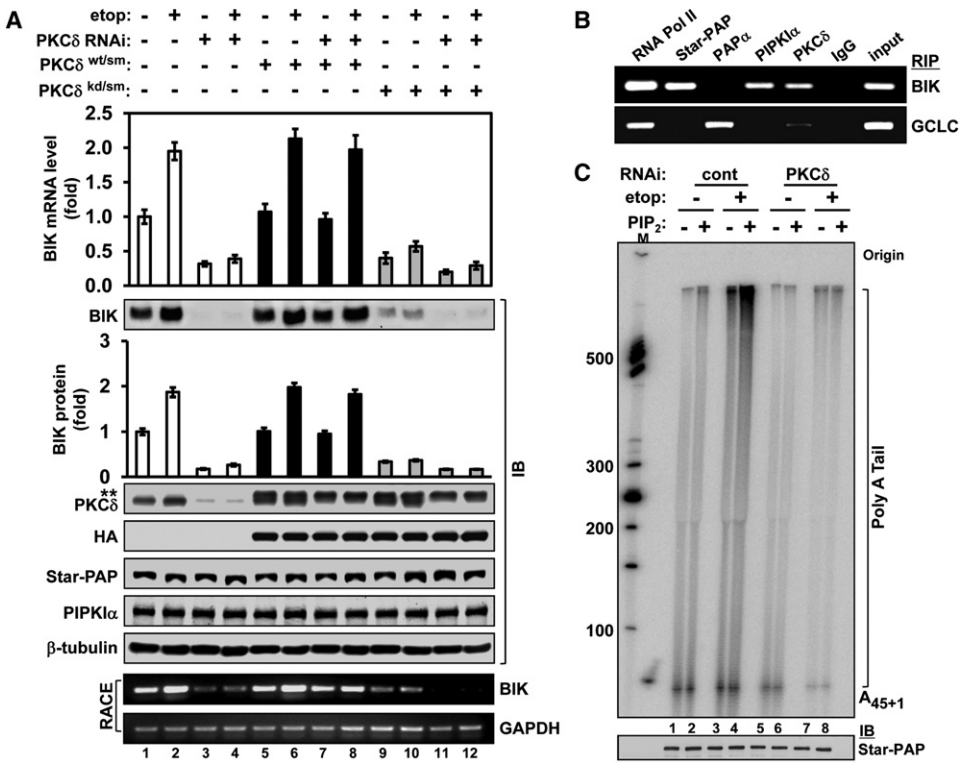

Figure 5. PKCδ Regulates Star-PAP Activity and *BIK* Expression and Associates with *BIK* mRNA

(A) RNAi knockdown of PKCδ reduced the basal and etoposide-potentiated *BIK* mRNA levels (top panel) as well as protein levels (middle panels). Expressing the wild-type (wt) but not the kinase dead (kd) *PKCδ* with silent mutations (sm) (**) for RNAi restored the decreased BIK levels induced by PKCδ knockdown. A similar expression pattern was shown for the 3′ RACE experiments (bottom panels). Error bars for mRNA expression represent SEM of three independent experiments with triplicate for each experimental condition. Error bars for protein quantification represent standard deviation, n = 3 independent experiments.

(B) RIP identified the specific presence of Star-PAP, PIPKIα, and PKCδ but not PAPα on the *BIK* mRNA, while PAPα showed specific association with the *GCLC* RNA. *RNA Pol II* was used as a positive control and the nonimmune IgG as a negative control.

(C) PKCδ knockdown efficiently blocked Star-PAP in vitro poly(A) polymerase activity induced by etoposide ± PI4,5P$_2$. M = Marker, shows units of the length of the extended A's. The loading control of total Star-PAP protein used for each experimental condition was checked by IB. See also Figures S4 and S5.

(Figure 5B). In contrast, PAPα was associated with the Star-PAP nontarget *GCLC* RNA, but not with *BIK* RNA. PIPKIα was also not associated with *GCLC* RNA, whereas PKCδ showed weak association (Figure 5B), indicating that *BIK* mRNA is a selective target for the Star-PAP pre-mRNA processing complex.

To further explore whether PKCδ directly modulates Star-PAP poly(A) polymerase activity, Star-PAP was affinity-purified from the cells stably expressing FLAG-Star-PAP with or without PKCδ knockdown or/and etoposide treatment (Figures S4B and S4C). The purified Star-PAP was used in the in vitro poly(A) polymerase assays as previously described (Mellman et al., 2008). Upon DNA damage (etoposide treatment), the poly(A) polymerase activity of Star-PAP was stimulated and the addition of PI4,5P$_2$ further enhanced this activity (Figure 5C). Star-PAP poly(A) polymerase activity under these conditions was highly processive adding >600 adenine residues after initiation (Figure S5B). Nevertheless, Star-PAP has linear enzyme kinetics in its polyadenylation activity over this time range (data not shown). The PI4,5P$_2$ stimulation of Star-PAP activity also required priming by etoposide treatment (Figure 5C). Remarkably, PKCδ was required for Star-PAP activation, as knockdown of PKCδ (Figure S4B) blocked both the DNA damage stimulation and the priming required for PI4,5P$_2$ stimulation of Star-PAP activity (Figure 5C). These results were confirmed by assaying at the varying concentrations of Star-PAP purified from cells that were ± PKCδ RNAi in the presence or absence of etoposide treatment (Figure S5A). The combined data demonstrate that PKCδ is required for Star-PAP activity toward *BIK* downstream of DNA damage stimulation.

Star-PAP Binds to the *BIK* 3′ UTR RNA

Star-PAP directly binds to its target *HO-1* pre-mRNA in the UTR upstream of the poly(A) signal and recruits the cleavage and polyadenylation specificity factor (CPSF) 160 and 73 subunits (Laishram and Anderson, 2010). Since Star-PAP associated with the *BIK* mRNA in vivo, a direct interaction was explored. A fragment of *BIK* 3′ UTR RNA (−145 to +120 with respect to cleavage site), containing the *cis*-regulatory elements and the equivalent Star-PAP regulatory region as identified in *HO-1*, and an RNA fragment from the equivalent

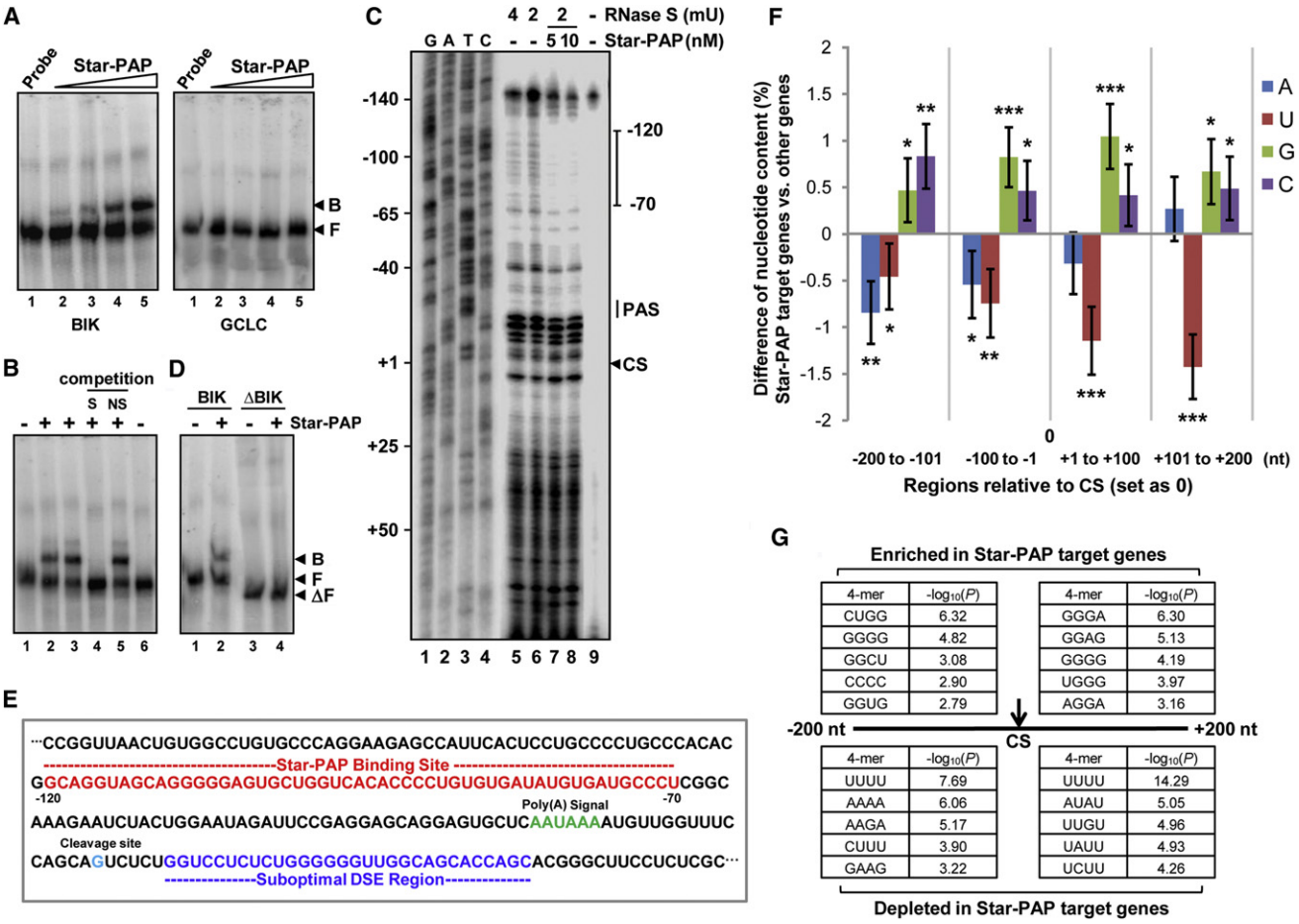

Figure 6. Star-PAP Binding Region in *BIK* UTR and the Sequence Analysis of Star-PAP Target UTRs

(A) RNA EMSA of *BIK* or *GCLC* with increasing concentrations of recombinant His-Star-PAP (0–30 nM). The control RNA (Probe), unbound RNA (F), and Star-PAP-RNA complex (B) are indicated.

(B) Cold competitions of *BIK* RNA binding with Star-PAP. EMSA of *BIK* RNA with Star-PAP (lanes 2 and 3) and 20-fold molar excess of the respective specific (S) and nonspecific (NS) competitor RNAs as indicated (lanes 4 and 5).

(C) Footprint of Star-PAP on *BIK* UTR RNA by RNase S probing. The digestion pattern with different RNase S concentrations (mU) in absence of Star-PAP (lanes 5 and 6) or in presence of 5 or 10 nM Star-PAP (lanes 7 and 8) and the untreated *BIK* RNA (lane 9) are indicated. Sequencing ladder is shown in lanes 1–4. Numbers on the left refer to the position of nucleotides with respect to cleavage site (CS). PAS = poly(A) signal.

(D) RNA EMSA of *BIK* UTR RNA deleted for the Star-PAP protection site (lanes 3 and 4) and control with *BIK* UTR RNA (lanes 1 and 2).

(E) The primary region of Star-PAP protection (red) on *BIK* UTR RNA and the *cis*-elements of *BIK* 3′ end UTR. The poly(A) signal (green), cleavage site (light blue), and suboptimal DSE (blue) are indicated.

(F) Biased nucleotide composition around the cleavage site in Star-PAP target compared to nontarget genes. The proportional test was used to examine whether the difference in nucleotide composition is significant. *$p < 5 \times 10^{-2}$; **$p < 1 \times 10^{-4}$; ***$p < 1 \times 10^{-6}$. Error bars are 95% confidence interval.

(G) *Cis*-element analysis around the cleavage site in Star-PAP targeted genes. The 200 nucleotide (nt) regions upstream and downstream of each cleavage site were used for analysis. The top five 4-mers for each region by the Fisher's exact test are shown. Their p values are also indicated. See also Figure S6.

region of the Star-PAP nontarget gene *GCLC* were transcribed. In vitro RNA electrophoretic mobility shift assays (EMSA) using radiolabeled *BIK* or *GCLC* UTR RNA were carried out. A slower migrating binary complex of Star-PAP and *BIK* RNA was detected with increasing Star-PAP concentration, but there was no detectable interaction with the *GCLC* RNA (Figure 6A). This *BIK* RNA fragment was also confirmed as the minimum upstream sequence from the *BIK* cleavage site that show optimum binding to Star-PAP by deletion analysis of the *BIK* UTR (data not shown).

In competition experiments, the Star-PAP-*BIK* RNA complex was competed with 20-fold molar excess of cold *BIK* UTR RNA but not by a nonspecific RNA of similar length (Figure 6B). Addition of Star-PAP antibody but not a control antibody resulted in a supershift of the Star-PAP-*BIK* RNA complex (Figure S6A). PAPα did not bind to the *BIK* RNA at similar concentrations to that of Star-PAP (data not shown). These results are consistent with the RIP data (Figure 5B) and with previous reports that PAPα has low affinity for RNA (Wahle, 1991), and they demonstrate that Star-PAP

directly and specifically interacts with the 3′ UTR of the *BIK* pre-mRNA.

To map the Star-PAP binding region on the *BIK* UTR, an RNA footprinting assay was employed using the *BIK* UTR RNA substrate used in EMSA experiments. A ladder of digested fragments of BIK RNA was generated with different concentrations of RNase S (Figure 6C, lanes 5 and 6). The site of protection by Star-PAP binding was obtained after comparing with that received His-Star-PAP (Figure 6C, lanes 7 and 8). Several positions within the *BIK* UTR were specifically protected by Star-PAP against RNase S cleavage. The protected region extended from ~120 to ~70 nucleotides upstream of the cleavage site (taken as +1) with a Star-PAP dose dependency for protection (Figure 6C). A similar result was also observed from footprinting with RNase T1 (Figure S6C). The putative Star-PAP binding region on *BIK* UTR RNA was deleted and reassayed for binding using EMSA. The results showed that Star-PAP did not bind the *BIK* RNA lacking this region (Figure 6D). These data defined the Star-PAP binding sequence in *BIK* UTR (Figure 6E).

The *BIK* UTR Sequence Suggests a Mechanism for Star-PAP Specificity

Comparison of the Star-PAP binding regions in *BIK* and *HO-1* UTR showed similar nucleotide sequences with high GC contents (>65%) (Figure S6B). Using a bioinformatics approach, the UTR sequences of all genes that were downregulated by Star-PAP knockdown in the microarray analysis (Mellman et al., 2008) were analyzed. This demonstrated that there is an enrichment of G and C nucleotides upstream of cleavage site in the putative Star-PAP target mRNAs compared to the UTRs of Star-PAP nonregulated genes (Figure 6F). In addition, we observed enrichment of G-rich 4-mers (CUGG, GGGG, GGGA, GGAG, etc.) around the cleavage site of Star-PAP targets (Figure 6G). This is consistent with the Star-PAP footprint on *HO-1* and *BIK*, and indicates that Star-PAP directly binds GC-rich sequence upstream of the poly(A) signal.

Most interestingly, this analysis showed a deficiency in U-content 3′ to cleavage site among the Star-PAP target genes, especially in the region of downstream sequence elements (DSE) (Figure 6F). This is important because CstF complex recognizes the U-rich or GU-rich DSE and cooperates with CPSF-160 binding to form a stable cleavage complex, required for canonical 3′ end processing (Murthy and Manley, 1995; Zhao et al., 1999). Our analysis also revealed that U-rich 4-mers (UUUU, UAUU, UUGU, etc.) were highly depleted in this region (Figure 6G) among the Star-PAP targets. Markedly, sequence analysis of the *BIK* UTR sequence demonstrated that in addition to the high GC-rich Star-PAP binding region upstream of the poly(A) signal, there was no U/GU-rich consensus or optimal DSE for CstF binding 3′ to cleavage site (Figure 6E). This indicates that the deficiency of a CstF binding region might render the canonical PAPα-based 3′ end processing complex unable to access *BIK* and potentially other Star-PAP target mRNAs. As Star-PAP functions distinctly by directly binding and recruiting the CPSF 160 and 73 subunits to the RNA (Laishram and Anderson, 2010), this may reduce the requirement for CstF binding.

Star-PAP Is Required for DNA Damage-Induced Apoptosis

PKCδ and BIK play key roles in apoptosis (Chinnadurai et al., 2008; Humphries et al., 2006; Reyland, 2007). As nuclear PIPKIα and PKCδ regulate Star-PAP-control of *BIK* mRNA processing and expression, Star-PAP may regulate the apoptotic response to DNA damage. To test this hypothesis, total genomic DNA was extracted from cells treated with or without Star-PAP knockdown or/and etoposide and assayed for DNA laddering indicative of chromatin DNA fragmentation. In non-etoposide-treated cells, basal DNA fragmentation level was observed and reduced in Star-PAP knockdown cells (Figure 7A). Etoposide induced DNA fragmentation and this was blocked by Star-PAP knockdown (Figure 7A). These results were corroborated by an analysis of caspase 9 and caspase 3/7 activation. DNA damage-induced cellular caspase 9 and caspase 3/7 activities were abolished by loss of Star-PAP (Figure 7B). It was reported that a requirement of BIK for apoptosis is likely cell-type-dependent, and loss of another BH3-only protein BIM could impair the proapoptotic effect (Coultas et al., 2005). To examine the combined effect of the loss of BIK expression via the Star-PAP-controlled pathway and the loss BIM expression, Star-PAP and/or BIM were knocked down followed by etoposide treatment and specific caspase activities were measured. While single knockdown of Star-PAP or BIM could each reduce caspase 9 and caspase 3/7 activities in etoposide-treated cells, double knockdown of Star-PAP and BIM further prevented the apoptotic effect (Figure S7).

PKCδ Regulation of the Star-PAP Specificity and Activity Is Specific for DNA Damage but Not Oxidative Stress

Star-PAP regulates a subset of genes, including *HO-1*, that have roles in oxidative stress response (Laishram and Anderson, 2010; Mellman et al., 2008). PKCδ is reported to play roles in aspects of the oxidative stress response (Konishi et al., 1997). Yet, there is no evidence for PKCδ regulation of HO-1 expression. As PKCδ regulates Star-PAP in the DNA damage-induced BIK expression pathway, we examined if PKCδ is also required for oxidative stress-mediated Star-PAP regulation of BIK and HO-1 expression. While the oxidative stress agonist tBHQ induced dramatic increase in HO-1 protein level, the cellular BIK level remained unaffected (Figure 7C, lanes 1 and 5). As expected, Star-PAP or PIPKIα knockdown attenuated both HO-1 and BIK expression regardless of the presence of tBHQ (Figure 7C, lanes 2, 3, 6, and 7). Yet, knockdown of PKCδ diminished BIK but not HO-1 protein levels in both tBHQ non-treated and treated cells (Figure 7C, lanes 1, 4, 5, and 8).

Moreover, an in vitro poly(A) polymerase assay, using affinity-purified FLAG-Star-PAP from cells treated with or without PKCδ knockdown in the presence or absence of tBHQ or etoposide treatment, showed that while PKCδ knockdown blocked the etoposide priming of PI4,5P_2-stimulation of Star-PAP activity (Figure 7D, lanes 3, 4, 7, and 8), tBHQ- and PI4,5P_2-stimulated Star-PAP poly(A) polymerase activities were not impacted by the loss of PKCδ (Figure 7D, lanes 9, 10, 11, and 12). These data indicate that PKCδ regulation of Star-PAP activity is specific to the DNA damage-signaling pathway where Star-PAP regulates BIK expression.

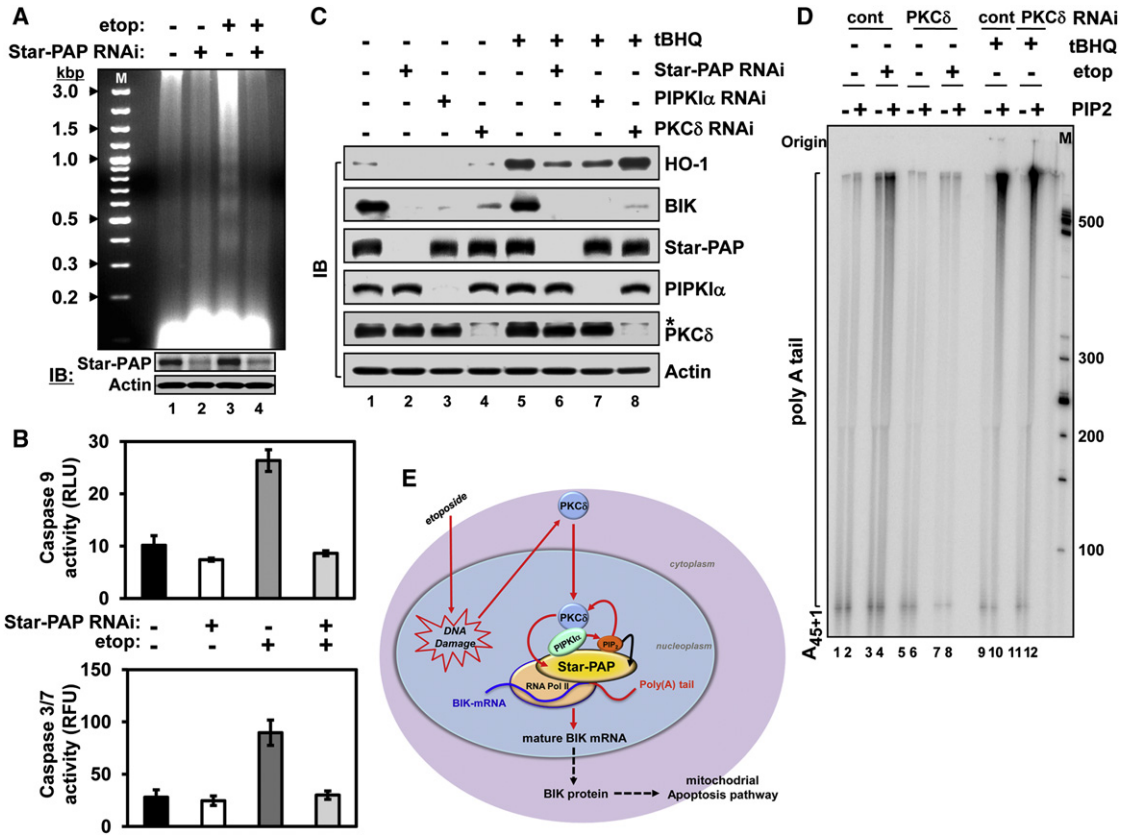

Figure 7. Star-PAP Is Required for Etoposide-Induced Apoptosis that Is Specifically Regulated by PKCδ

(A) DNA laddering assay demonstrated that knockdown of Star-PAP rescued etoposide-induced DNA fragmentation within the cells. M = Marker (DNA in kilobase pair). Efficiency of the knockdown is illustrated at the bottom panels.

(B) Star-PAP knockdown attenuated caspase activities induced by etoposide. RLU = relative luminescence unit. RFU = relative fluorescence unit. Error bars represent SEM of three independent experiments with triplicate for each experimental condition.

(C) PKCδ is not involved in oxidative stress-regulated HO-1 expression. BIK and HO-1 protein levels in cells treated with or without Star-PAP, PIPKIα, or PKCδ knockdown and tBHQ were analyzed by IB. * = nonspecific bands.

(D) In vitro poly(A) polymerase assay analyzing the effect of PKCδ knockdown on Star-PAP poly(A) polymerase activities in response to etoposide or tBHQ treatment.

(E) Model of the nuclear phosphoinositide signaling-regulated Star-PAP control of *BIK* expression. Etoposide-induced DNA damage signal stimulates the nuclear localization of PKCδ, which is then integrated into the Star-PAP complex and interacts with the PI4,5P$_2$-producing enzyme PIPKIα. The active PIPKIα generates PI4,5P$_2$ to activate PKCδ, which in turn promotes the activities of Star-PAP for the 3′ end processing of the *BIK* mRNA.

DISCUSSION

BIK expression is a key switch for the initiation of the mitochondrial apoptosis pathway. BIK is also recognized as a tumor suppressor (Chinnadurai et al., 2008) whose transcription is regulated in part by p53 (Hur et al., 2006; Mathai et al., 2002) and DNA damage stimuli (Real et al., 2006). Although the mechanisms for *BIK* transcription have been studied, the role of *BIK* 3′ end processing in its expression and translation remains uncharacterized. As BIK acts as an early initiator for apoptosis, the processing of the message is a fundamental step in the expression pathway.

Here, we have shown that Star-PAP controls the 3′ end cleavage and polyadenylation of the *BIK* pre-mRNA, a process essential for stability, export, and translation of the message. Although *BIK* 3′ UTR has an intact poly(A) signal (AAUAAA), it cannot be processed by the PAPα canonical 3′ end processing complex. PAPα has very low affinity for RNA substrate (Martin and Keller, 1996; Wahle, 1991) and lacks RNA binding specificity (Zhao et al., 1999). Thus, PAPα is recruited to pre-mRNA by the cooperative binding of CPSF to the poly(A) signal and CstF to a U/GU-rich element that is 3′ to the cleavage site (Keller et al., 1991; Murthy and Manley, 1995). There are examples of suboptimal poly(A) sequences, where an intact AAUAAA is not sufficient for the CPSF complex to bind the pre-mRNA and recruit PAPα (Gilmartin et al., 1995). There are also examples of suboptimal CstF U/GU-rich element sites (Hu et al., 2005; Maciolek and McNally, 2008; Tian et al., 2005).

Star-PAP directly binds to the 3′ end of pre-mRNAs upstream of the poly(A) signal (Figure 6). The Star-PAP protection region on both *BIK* and *HO-1* shows a high GC-rich sequence motif. Star-PAP interacts with RNA harboring multiple binding motifs

that have a relatively large footprint on the UTR. Star-PAP binding to the pre-mRNA recruits CPSF160 and CPSF73 by direct protein-protein interactions (Laishram and Anderson, 2010). Unlike canonical PAPα, Star-PAP, CPSF160, and CPSF73 are sufficient to reconstitute specific 3′ end cleavage in vitro, indicating that the CstF complex plays a less important role for Star-PAP targets (Laishram and Anderson, 2010). Thus, for some Star-PAP exclusive pre-mRNA targets a plausible explanation for loss of PAPα usage could be the loss of CPSF-CstF complex assembly onto the target mRNAs, resulting in deficient recruitment of PAPα to the pre-mRNAs. Sequence analysis of Star-PAP-regulated genes, including *BIK*, has demonstrated that apart from the GC-rich sequence around the cleavage site, there is depletion of U-rich sequence in the region of DSE resulting in a suboptimal CstF recognition site (Figure 6). The deficiency of CstF binding would impede both the stable assembly of CPSF-160 on the poly(A) signal and recruitment of PAPα to the cleavage site of *BIK* UTR. These changes could render *BIK* an exclusive Star-PAP target.

PKCδ is a central switch that controls the apoptosis pathway, and this requires the nuclear localization and cleavage of PKCδ by caspase-3 (Reyland, 2007). Yet, considerable evidence indicates that the full-length PKCδ initiates the apoptotic response to DNA damage and acts upstream of caspase-3 (Cataldi et al., 2002; Fujii et al., 2000; Humphries et al., 2006). Only the intact PKCδ was detected associated with the Star-PAP complex, indicating that PKCδ modulation of Star-PAP is an early event in the PKCδ response to DNA damage.

In the nucleus, the regulation of PKCδ by lipid messengers such as diacylglycerol (DAG) or phosphoinositides has not been defined. Our data supports a model where PKCδ is recruited to the Star-PAP complex by direct interaction with PIPKIα, and this interaction blocked PKCδ activity, but PI4,5P_2 generated by PIPKIα stimulated PKCδ activity even in the presence of PIPKIα (Figure 7E). This regulatory mechanism for PKCδ is unexpected, with the potential for utilization in other PIPKIα- and PKCδ-regulated pathways. PKCδ phosphorylates Star-PAP, and perhaps other components in the complex, to regulate *BIK* pre-mRNA 3′ end processing. The data also demonstrate that DNA damage-induced PKCδ activity is required for the priming of Star-PAP such that PI4,5P_2 generated by PIPKIα can stimulate Star-PAP poly(A) polymerase activity (Figure 5C).

PKCδ can also be activated by DAG that is generated by nuclear phosphoinositide-phospholipase C toward PI4,5P_2 (Stahelin et al., 2004). We showed that the DAG analog PMA stimulated PKCδ phosphorylation of Star-PAP (Figure 2E). However, the PKCδ phosphorylation of Star-PAP was blocked by PIPKIα binding and relieved by PI4,5P_2 but not PMA. This indicates that in vivo PI4,5P_2 and not DAG modulates PKCδ in the Star-PAP pathway that controls BIK expression.

The 3′ end processing of *BIK* requires a Star-PAP-dependent signaling nexus that contains at least two key signaling enzymes —PIPKIα, which generates PI4,5P_2, and PKCδ, which is regulated by direct binding of PIPKIα and PI4,5P_2 stimulation. *BIK* and *HO-1* are exclusive Star-PAP target genes that are both regulated by PIPKIα and PI4,5P_2, but the BIK expression pathway is in addition controlled by PKCδ. This is the first indication that distinct signaling pathways that utilize different signaling enzymes regulate Star-PAP control of gene expression. The identification of PKCδ as a component of this nexus integrates Star-PAP, PKCδ, PIPKIα, and PI4,5P_2 into a signaling pathway essential for *BIK* expression and initiation of apoptosis, and therefore has wide ramifications for mRNA processing and gene expression.

EXPERIMENTAL PROCEDURES

Cell Lines, Transfection, and Treatments

Human embryonic kidney (HEK) 293 cells were obtained from American Type Culture Collection (ATCC) and cultured in 1× DMEM supplemented with 10% fetal bovine serum and penicillin/streptomycin (50 U/ml) and were grown at 37°C in 5% CO_2. Transfection with the plasmids and the siRNAs (Supplemental Information) was performed as described (Mellman et al., 2008). Whenever required, cells were treated with 100 μM etoposide/tBHQ or the vehicle control, DMSO, for 4 hr or prolonged time as indicated and harvested for analysis.

Quantitative Real-Time RT-PCR

Total RNA was extracted and reverse transcribed. Target mRNA was quantified with the MyiQ single-color real-time PCR detection system (Bio-Rad) as described previously (Mellman et al., 2008). Single-product amplification was confirmed by melting-curve analysis, and primer efficiency was near 100% in all experiments. Target mRNA abundance was normalized to *GAPDH* expression. Primers used for mRNA expression and 3′ end cleavage are shown in Supplemental Information.

Immunoblot, Immunoprecipitation, and Antibodies

IB and IP were carried out as described (Mellman et al., 2008). The intensity of the bands on images was quantified using ImageJ software. Input = 10% of the total protein used for the IP. The antibodies used are shown in Supplemental Information.

Protein Kinase Assay

The kinase assay was performed as detailed in the Supplemental Information.

Immunofluorescence Microscopy

This was performed as previously described (Boronenkov et al., 1998). The ratios for comparing protein associations were generated by computerized counting of the overlaid yellow spots in 20 cells for each assay condition from a representative experiment.

GST Pull-Down Assay

Human recombinant GST-tagged PKCδ (echelon, #E-K037) and His-tagged Star-PAP or PIPKIα (affinity purified) were subjected to GST pull-down assay as described previously (Ling et al., 2007). Input = 1% of the total protein used for the pull-down.

RNA Immunoprecipitation

RIP was performed as described (Mellman et al., 2008), using antibodies against endogenous RNA Pol II, Star-PAP, PAPα, PIPKIα, and PKCδ. The primers used to detect the *BIK* or *GCLC* UTR are shown in Supplemental Information.

3′ RACE and mRNA 3′ End Cleavage Measurement

3′ RACE was performed with the GeneRacer system (Invitrogen, #L1502-01) using *BIK* or *GAPDH* gene-specific primers and the 3′ adapter primer, following the manufacturer's instructions. PCR products were run on agarose gel, and individual DNA bands were excised, purified, and ligated into the pGEM-T Easy Vector (Promega, #A1360) for sequencing. For the 3′ end cleavage, total RNA was isolated and the uncleaved pre-mRNA level was measured by real-time PCR, as described (Mellman et al., 2008). The

noncleaved message was represented as fold over the total mRNA and normalized against the nontreated control sample.

Poly(A) Polymerase Assay

The FLAG-tagged Star-PAP was affinity purified, and the poly(A) polymerase assay was carried out using the 45-mer RNA oligonucleotide $(UAGGGA)_5A_{15}$ as an RNA substrate, as described previously (Mellman et al., 2008).

RNA EMSA and RNase Footprinting

Uniformly radiolabeled *BIK* UTR RNA substrates were prepared by run-off in vitro transcription from the linearized plasmid pTZ-*BIK* (harbors T7 promoter and *BIK* 3′ UTR) using the T7 transcription Kit (Fermentas). EMSA was carried out in 20 μl EMSA binding buffer, as described (Laishram and Anderson, 2010). The RNA Footprinting was carried out as detailed in the Supplemental Information.

Sequence Analysis of Star-PAP Target Gene UTRs

The microarray data for Star-PAP knockdown in HEK293 cells (Mellman et al., 2008) were analyzed. Cleavage site information was obtained from PolyA_DB (Lee et al., 2007). The Robust Multichip Average (RMA) method was used for data normalization, and the cutoff of p value < 0.05 (t test) and fold change > 1.5 was used to select genes showing significant downregulation, which were considered as Star-PAP targets. Those with one poly(A) signal only as based on the cDNA and EST evidence were used for nucleotide and *cis*-element analyses. The proportional test and the Fisher's exact test were used to assess the difference in nucleotide content and the significance of 4-mers in different regions surrounding cleavage sites, respectively.

DNA Laddering Assay

The assay was performed as described (Gong et al., 1994). Equal amounts of cells from each experimental condition were collected 24 hr after etoposide treatment and fixed with ice-cold 70% ethanol. DNA was extracted using phosphate-citrate buffer, treated with RNase and proteinase K, and analyzed by agarose gel electrophoresis.

Detection of Caspase Activities

Caspase activities under the experimental conditions were measured using commercially available assay kits as described in the Supplemental Information.

SUPPLEMENTAL INFORMATION

Supplemental Information includes seven figures, Supplemental Experimental Procedures, and Supplemental References and can be found with this article online at doi:10.1016/j.molcel.2011.11.017.

ACKNOWLEDGMENTS

The authors thank Shigeki Miyamoto, Randal Tibbetts, and Jay Yang for comments. This study was supported by an NIH grant (GM051968) to R.A.A.; an NIH grant (GM084089) to B.T.; an AHA Postdoctoral Fellowship (0920072G) to R.S.L.; and a Ruth L. Kirschstein National Research Service Award (F32 G082005) to C.A.B.

Received: January 19, 2011
Revised: June 3, 2011
Accepted: November 4, 2011
Published: January 12, 2012

REFERENCES

Baldwin, E.L., and Osheroff, N. (2005). Etoposide, topoisomerase II and cancer. Curr. Med. Chem. Anticancer Agents *5*, 363–372.

Barlow, C.A., Laishram, R.S., and Anderson, R.A. (2010). Nuclear phosphoinositides: a signaling enigma wrapped in a compartmental conundrum. Trends Cell Biol. *20*, 25–35.

Blass, M., Kronfeld, I., Kazimirsky, G., Blumberg, P.M., and Brodie, C. (2002). Tyrosine phosphorylation of protein kinase Cdelta is essential for its apoptotic effect in response to etoposide. Mol. Cell. Biol. *22*, 182–195.

Boronenkov, I.V., Loijens, J.C., Umeda, M., and Anderson, R.A. (1998). Phosphoinositide signaling pathways in nuclei are associated with nuclear speckles containing pre-mRNA processing factors. Mol. Biol. Cell *9*, 3547–3560.

Brodie, C., and Blumberg, P.M. (2003). Regulation of cell apoptosis by protein kinase c delta. Apoptosis *8*, 19–27.

Brose, N., and Rosenmund, C. (2002). Move over protein kinase C, you've got company: alternative cellular effectors of diacylglycerol and phorbol esters. J. Cell Sci. *115*, 4399–4411.

Cataldi, A., Miscia, S., Centurione, L., Rapino, M., Bosco, D., Grifone, G., Valerio, V.D., Garaci, F., and Rana, R. (2002). Role of nuclear PKC delta in mediating caspase-3-upregulation in Jurkat T leukemic cells exposed to ionizing radiation. J. Cell. Biochem. *86*, 553–560.

Chauhan, V.P., and Brockerhoff, H. (1988). Phosphatidylinositol-4,5-bisphosphate may antecede diacylglycerol as activator of protein kinase C. Biochem. Biophys. Res. Commun. *155*, 18–23.

Chinnadurai, G., Vijayalingam, S., and Rashmi, R. (2008). BIK, the founding member of the BH3-only family proteins: mechanisms of cell death and role in cancer and pathogenic processes. Oncogene *27* (*Suppl 1*), S20–S29.

Cocco, L., Gilmour, R.S., Ognibene, A., Letcher, A.J., Manzoli, F.A., and Irvine, R.F. (1987). Synthesis of polyphosphoinositides in nuclei of Friend cells. Evidence for polyphosphoinositide metabolism inside the nucleus which changes with cell differentiation. Biochem. J. *248*, 765–770.

Coultas, L., Bouillet, P., Loveland, K.L., Meachem, S., Perlman, H., Adams, J.M., and Strasser, A. (2005). Concomitant loss of proapoptotic BH3-only Bcl-2 antagonists Bik and Bim arrests spermatogenesis. EMBO J. *24*, 3963–3973.

DeVries, T.A., Neville, M.C., and Reyland, M.E. (2002). Nuclear import of PKCdelta is required for apoptosis: identification of a novel nuclear import sequence. EMBO J. *21*, 6050–6060.

Fu, Y., Li, J., and Lee, A.S. (2007). GRP78/BiP inhibits endoplasmic reticulum BIK and protects human breast cancer cells against estrogen starvation-induced apoptosis. Cancer Res. *67*, 3734–3740.

Fujii, T., García-Bermejo, M.L., Bernabó, J.L., Caamaño, J., Ohba, M., Kuroki, T., Li, L., Yuspa, S.H., and Kazanietz, M.G. (2000). Involvement of protein kinase C delta (PKCdelta) in phorbol ester-induced apoptosis in LNCaP prostate cancer cells. Lack of proteolytic cleavage of PKCdelta. J. Biol. Chem. *275*, 7574–7582.

Germain, M., Mathai, J.P., and Shore, G.C. (2002). BH-3-only BIK functions at the endoplasmic reticulum to stimulate cytochrome c release from mitochondria. J. Biol. Chem. *277*, 18053–18060.

Ghayur, T., Hugunin, M., Talanian, R.V., Ratnofsky, S., Quinlan, C., Emoto, Y., Pandey, P., Datta, R., Huang, Y., Kharbanda, S., et al. (1996). Proteolytic activation of protein kinase C delta by an ICE/CED 3-like protease induces characteristics of apoptosis. J. Exp. Med. *184*, 2399–2404.

Gilmartin, G.M., Fleming, E.S., Oetjen, J., and Graveley, B.R. (1995). CPSF recognition of an HIV-1 mRNA 3′-processing enhancer: multiple sequence contacts involved in poly(A) site definition. Genes Dev. *9*, 72–83.

Gong, J., Traganos, F., and Darzynkiewicz, Z. (1994). A selective procedure for DNA extraction from apoptotic cells applicable for gel electrophoresis and flow cytometry. Anal. Biochem. *218*, 314–319.

Gonzales, M.L., and Anderson, R.A. (2006). Nuclear phosphoinositide kinases and inositol phospholipids. J. Cell. Biochem. *97*, 252–260.

Gonzales, M.L., Mellman, D.L., and Anderson, R.A. (2008). CKIalpha is associated with and phosphorylates star-PAP and is also required for expression of select star-PAP target messenger RNAs. J. Biol. Chem. *283*, 12665–12673.

Han, J., Sabbatini, P., and White, E. (1996). Induction of apoptosis by human Nbk/Bik, a BH3-containing protein that interacts with E1B 19K. Mol. Cell. Biol. *16*, 5857–5864.

Heck, J.N., Mellman, D.L., Ling, K., Sun, Y., Wagoner, M.P., Schill, N.J., and Anderson, R.A. (2007). A conspicuous connection: structure defines function for the phosphatidylinositol-phosphate kinase family. Crit. Rev. Biochem. Mol. Biol. *42*, 15–39.

Hu, J., Lutz, C.S., Wilusz, J., and Tian, B. (2005). Bioinformatic identification of candidate cis-regulatory elements involved in human mRNA polyadenylation. RNA *11*, 1485–1493.

Huang, F.L., and Huang, K.P. (1991). Interaction of protein kinase C isozymes with phosphatidylinositol 4,5-bisphosphate. J. Biol. Chem. *266*, 8727–8733.

Humphries, M.J., Limesand, K.H., Schneider, J.C., Nakayama, K.I., Anderson, S.M., and Reyland, M.E. (2006). Suppression of apoptosis in the protein kinase Cdelta null mouse in vivo. J. Biol. Chem. *281*, 9728–9737.

Hur, J., Bell, D.W., Dean, K.L., Coser, K.R., Hilario, P.C., Okimoto, R.A., Tobey, E.M., Smith, S.L., Isselbacher, K.J., and Shioda, T. (2006). Regulation of expression of BIK proapoptotic protein in human breast cancer cells: p53-dependent induction of BIK mRNA by fulvestrant and proteasomal degradation of BIK protein. Cancer Res. *66*, 10153–10161.

Keller, W., Bienroth, S., Lang, K.M., and Christofori, G. (1991). Cleavage and polyadenylation factor CPF specifically interacts with the pre-mRNA 3′ processing signal AAUAAA. EMBO J. *10*, 4241–4249.

Konishi, H., Tanaka, M., Takemura, Y., Matsuzaki, H., Ono, Y., Kikkawa, U., and Nishizuka, Y. (1997). Activation of protein kinase C by tyrosine phosphorylation in response to H2O2. Proc. Natl. Acad. Sci. USA *94*, 11233–11237.

Laishram, R.S., and Anderson, R.A. (2010). The poly A polymerase Star-PAP controls 3′-end cleavage by promoting CPSF interaction and specificity toward the pre-mRNA. EMBO J. *29*, 4132–4145.

Laishram, R.S., Barlow, C.A., and Anderson, R.A. (2011). CKI isoforms α and ε regulate Star-PAP target messages by controlling Star-PAP poly(A) polymerase activity and phosphoinositide stimulation. Nucleic Acids Res. *39*, 7961–7973.

Lee, M.H., and Bell, R.M. (1991). Mechanism of protein kinase C activation by phosphatidylinositol 4,5-bisphosphate. Biochemistry *30*, 1041–1049.

Lee, J.Y., Yeh, I., Park, J.Y., and Tian, B. (2007). PolyA_DB 2: mRNA polyadenylation sites in vertebrate genes. Nucleic Acids Res. *35* (Database issue), D165–D168.

Ling, K., Bairstow, S.F., Carbonara, C., Turbin, D.A., Huntsman, D.G., and Anderson, R.A. (2007). Type I gamma phosphatidylinositol phosphate kinase modulates adherens junction and E-cadherin trafficking via a direct interaction with mu 1B adaptin. J. Cell Biol. *176*, 343–353.

Maciolek, N.L., and McNally, M.T. (2008). Characterization of Rous sarcoma virus polyadenylation site use in vitro. Virology *374*, 468–476.

Marshansky, V., Wang, X., Bertrand, R., Luo, H., Duguid, W., Chinnadurai, G., Kanaan, N., Vu, M.D., and Wu, J. (2001). Proteasomes modulate balance among proapoptotic and antiapoptotic Bcl-2 family members and compromise functioning of the electron transport chain in leukemic cells. J. Immunol. *166*, 3130–3142.

Martin, G., and Keller, W. (1996). Mutational analysis of mammalian poly(A) polymerase identifies a region for primer binding and catalytic domain, homologous to the family X polymerases, and to other nucleotidyltransferases. EMBO J. *15*, 2593–2603.

Mathai, J.P., Germain, M., Marcellus, R.C., and Shore, G.C. (2002). Induction and endoplasmic reticulum location of BIK/NBK in response to apoptotic signaling by E1A and p53. Oncogene *21*, 2534–2544.

Mellman, D.L., Gonzales, M.L., Song, C., Barlow, C.A., Wang, P., Kendziorski, C., and Anderson, R.A. (2008). A PtdIns4,5P2-regulated nuclear poly(A) polymerase controls expression of select mRNAs. Nature *451*, 1013–1017.

Murthy, K.G., and Manley, J.L. (1995). The 160-kD subunit of human cleavage-polyadenylation specificity factor coordinates pre-mRNA 3′-end formation. Genes Dev. *9*, 2672–2683.

Real, P.J., Sanz, C., Gutierrez, O., Pipaon, C., Zubiaga, A.M., and Fernandez-Luna, J.L. (2006). Transcriptional activation of the proapoptotic bik gene by E2F proteins in cancer cells. FEBS Lett. *580*, 5905–5909.

Reyland, M.E. (2007). Protein kinase Cdelta and apoptosis. Biochem. Soc. Trans. *35*, 1001–1004.

Rybin, V.O., Guo, J., Sabri, A., Elouardighi, H., Schaefer, E., and Steinberg, S.F. (2004). Stimulus-specific differences in protein kinase C delta localization and activation mechanisms in cardiomyocytes. J. Biol. Chem. *279*, 19350–19361.

Stahelin, R.V., Digman, M.A., Medkova, M., Ananthanarayanan, B., Rafter, J.D., Melowic, H.R., and Cho, W. (2004). Mechanism of diacylglycerol-induced membrane targeting and activation of protein kinase Cdelta. J. Biol. Chem. *279*, 29501–29512.

Steinberg, S.F. (2004). Distinctive activation mechanisms and functions for protein kinase Cdelta. Biochem. J. *384*, 449–459.

Tabellini, G., Bortul, R., Santi, S., Riccio, M., Baldini, G., Cappellini, A., Billi, A.M., Berezney, R., Ruggeri, A., Cocco, L., and Martelli, A.M. (2003). Diacylglycerol kinase-theta is localized in the speckle domains of the nucleus. Exp. Cell Res. *287*, 143–154.

Tanaka, Y., Gavrielides, M.V., Mitsuuchi, Y., Fujii, T., and Kazanietz, M.G. (2003). Protein kinase C promotes apoptosis in LNCaP prostate cancer cells through activation of p38 MAPK and inhibition of the Akt survival pathway. J. Biol. Chem. *278*, 33753–33762.

Tian, B., Hu, J., Zhang, H., and Lutz, C.S. (2005). A large-scale analysis of mRNA polyadenylation of human and mouse genes. Nucleic Acids Res. *33*, 201–212.

Wahle, E. (1991). Purification and characterization of a mammalian polyadenylate polymerase involved in the 3′ end processing of messenger RNA precursors. J. Biol. Chem. *266*, 3131–3139.

Yoshida, K. (2007). PKCdelta signaling: mechanisms of DNA damage response and apoptosis. Cell. Signal. *19*, 892–901.

Zhao, J., Hyman, L., and Moore, C. (1999). Formation of mRNA 3′ ends in eukaryotes: mechanism, regulation, and interrelationships with other steps in mRNA synthesis. Microbiol. Mol. Biol. Rev. *63*, 405–445.

Molecular Cell, Volume *45*

Supplemental Information

Star-PAP Control of BIK Expression and Apoptosis Is Regulated by Nuclear PIPKIα and PKCδ Signaling

Weimin Li, Rakesh S. Laishram, Zhe Ji, Christy A. Barlow, Bin Tian, and Richard A. Anderson

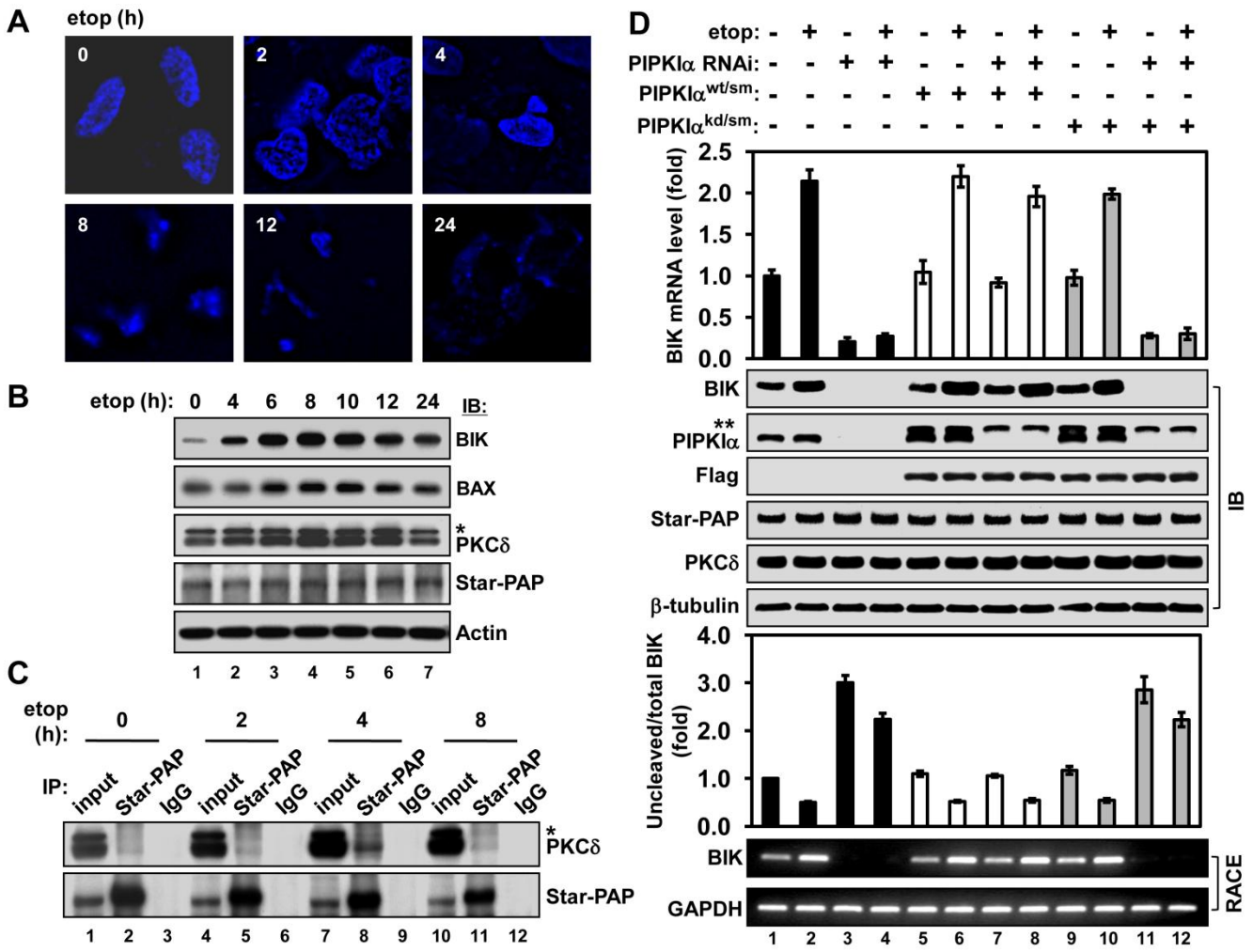

Figure S1. Effect of Etoposide on Nuclear DNA, Protein levels, PKCδ and Star-PAP Association, and Requirement of PIPKIα in *BIK* mRNA Expression

(A) IF staining of nuclear DNA with DAPI in cells treated with etoposide at different time points.

(B) BIK, BAX, PKCδ, and Star-PAP protein levels at different times (h = hour) of etoposide treatment.

(C) IP of Star-PAP from cells treated with etoposide and detection of PKCδ and Star-PAP levels with IB. ∗ = unspecific bands.

(D) PIPKIα kinase activity is required for BIK expression. Knockdown of PIPKIα abolished basal and etoposide-stimulated BIK mRNA and protein generation similar to the impact on *BIK* mRNA 3'-end cleavage and tail-message production, which were rescued by wild type but not kinase dead PIPKIα (∗∗). The Star-PAP non-target gene *GAPDH* was used as a negative control in the 3'-RACE assays. See also Figure 1 and Figure 4.

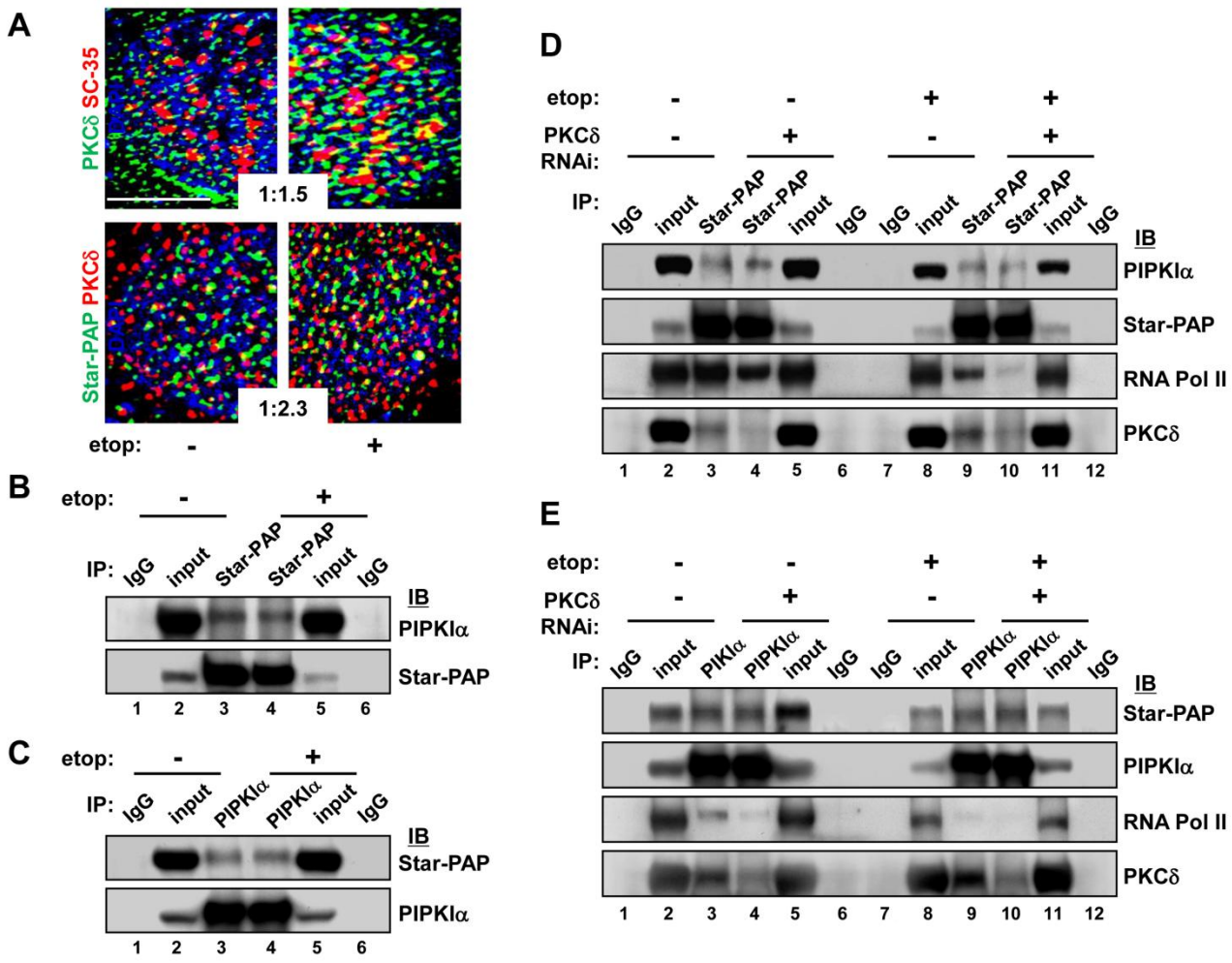

Figure S2. Etoposide Treatment Increased PKCδ and Star-PAP Association within the Cells but Resemble PKCδ Knockdown, Had No Effect on Star-PAP Association with PIPKIα

(A) IF staining showed enriched nuclear speckle occupancy of PKCδ and its association with Star-PAP after etoposide treatment. The fluorescent colors for PKCδ, SC-35, Star-PAP are indicated. The ratios (derived from image analysis with MetaMorph software) are for comparison of the merged yellow spots within nuclei between etoposide non-treated and treated cells. Scale bar = 10 μm.

(B–E) Star-PAP and PIPKIα association was neither affected by etoposide (B and C) nor by PKCδ knockdown (D and E) as evaluated by IP and IB. See also Figure 4.

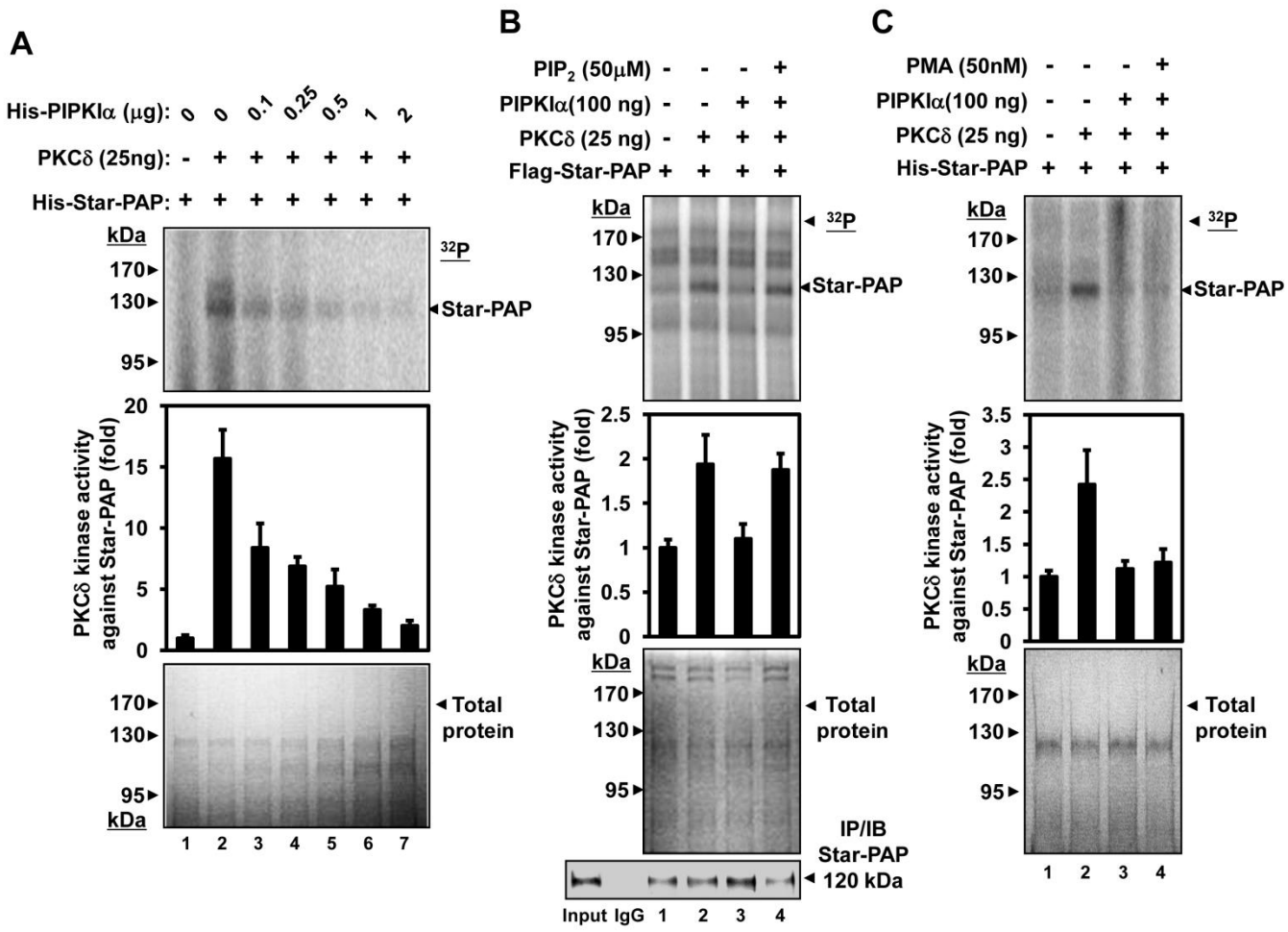

Figure S3. PIPKIα Inhibited PKCδ Phosphorylation of Star-PAP which Can Be Restored by PI4,5P$_2$ but Not PMA

(A) The PKCδ kinase activity against Star-PAP was quenched by adding PIPKIα.

(B) PIPKIα-blocked PKCδ phosphorylation of Flag-Star-PAP was rescued by PI4,5P$_2$. The band indicated as phosphorylated Star-PAP was further confirmed by IP and IB of Star-PAP from the denatured reaction mix.

(C) PMA failed to restore the PIPKIα-inhibited PKCδ kinase activity toward Star-PAP. Quantification of the kinase activities was normalized to the substrate-only lane. Total protein used in the kinase reaction was detected by Coomassie staining. See also Figure 4.

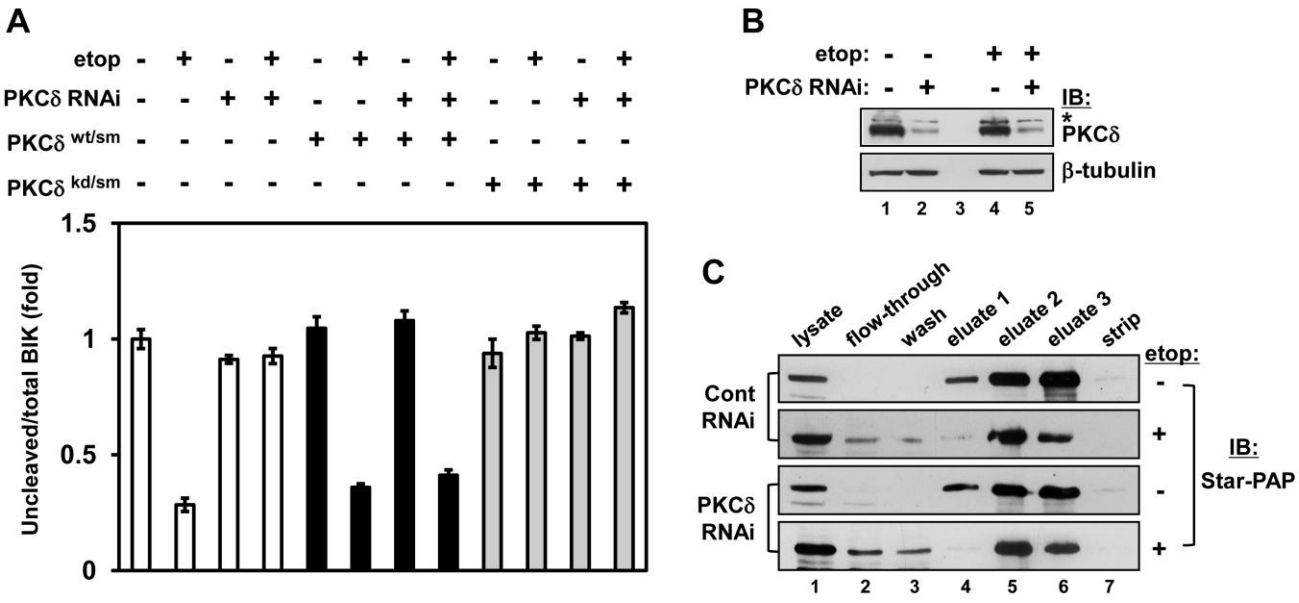

Figure S4. PKCδ Kinase Activity Is Required for *BIK* mRNA 3'-End Cleavage under DNA Damage Conditions

(A) Knockdown of PKCδ impaired the cleavage of *BIK* mRNA in the etoposide treated but not the non-treated cells. Overexpressing PKCδ$^{wt/sm}$ and not PKCδ$^{kd/sm}$ rescued the cleavage defect. Error bars represent SEM of 3 independent experiments with triplicate for each experimental condition.

(B) IB showing knockdown of PKCδ in presence or absence of etoposide treatment in Flag-Star-PAP stably expressing HEK 293 cells.

(C) The affinity purified Flag-tagged Star-PAP complexes from cells treated with or without PKCδ knockdown and etoposide (100 μM, 4 h) for in vitro poly(A) polymerase assays shown in Figure 5. ∗ = unspecific bands. See also Figure 5.

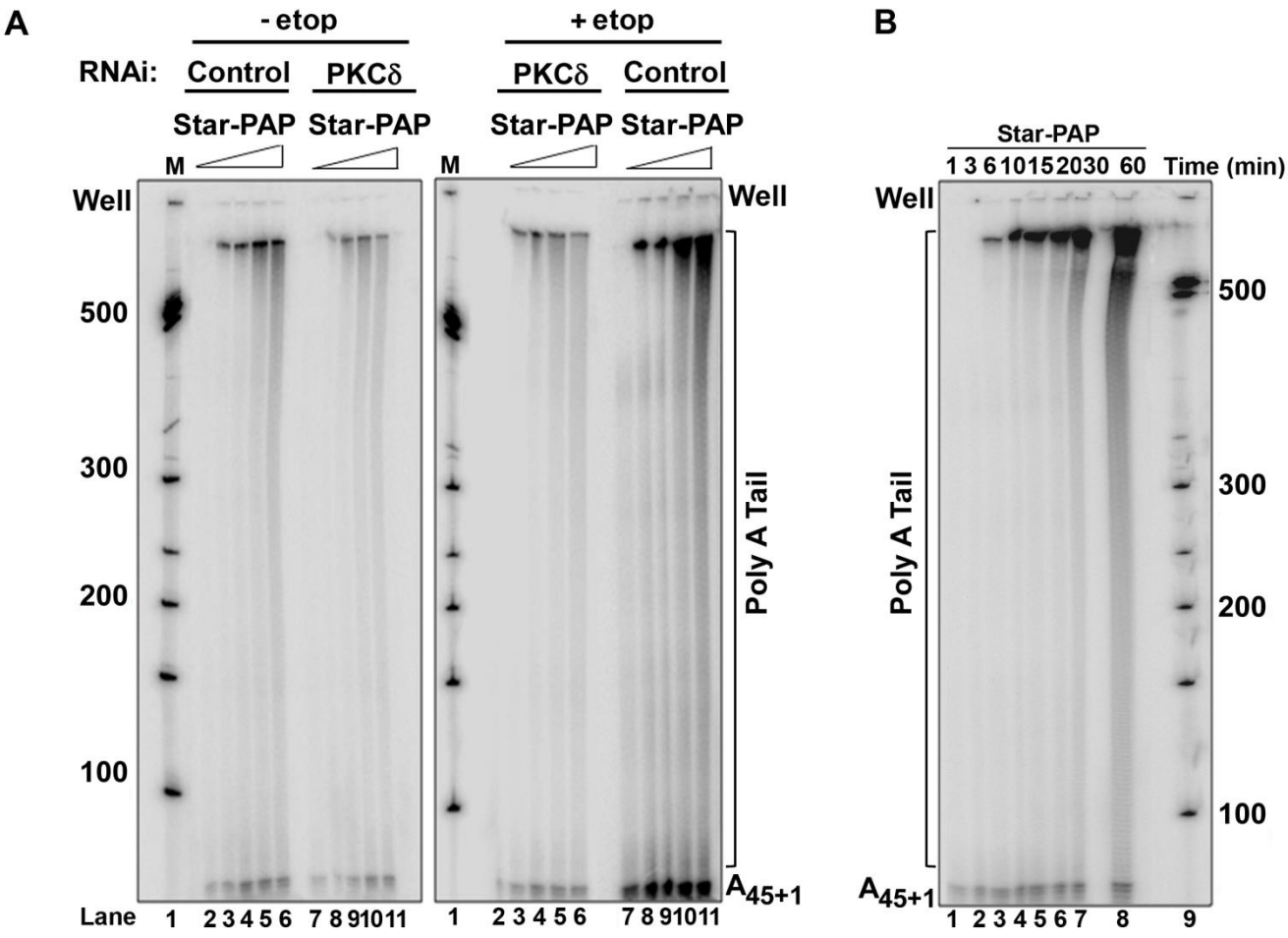

Figure S5. PKCδ Is Required for DNA Damage Signal-Mediated Star-PAP Polyadenylation Activities

(A) In vitro poly(A) polymerase assay in the presence of $PI4,5P_2$ using A_{45}-oligo and increasing concentrations of Flag-Star-PAP complex purified from HEK 293 cells stably expressing Flag-Star-PAP +/- PKCδ knockdown and with or without etoposide treatment. Star-PAP shows PKCδ-dependent polyadenylation of A_{45}-substrate and etoposide stimulates both initiation and processivity of Star-PAP polyadenylation.

(B) In vitro Star-PAP polyadenylation assay with A_{45}-oligos at increasing time points as indicated (1-60 min) in presence of $PI4,5P_2$. Quantification indicates a linear increase in Star-PAP polyadynylation activity with time (at least up to 60 min) (data not shown). The origin of the gel and markers are indicated. See also Figure 5.

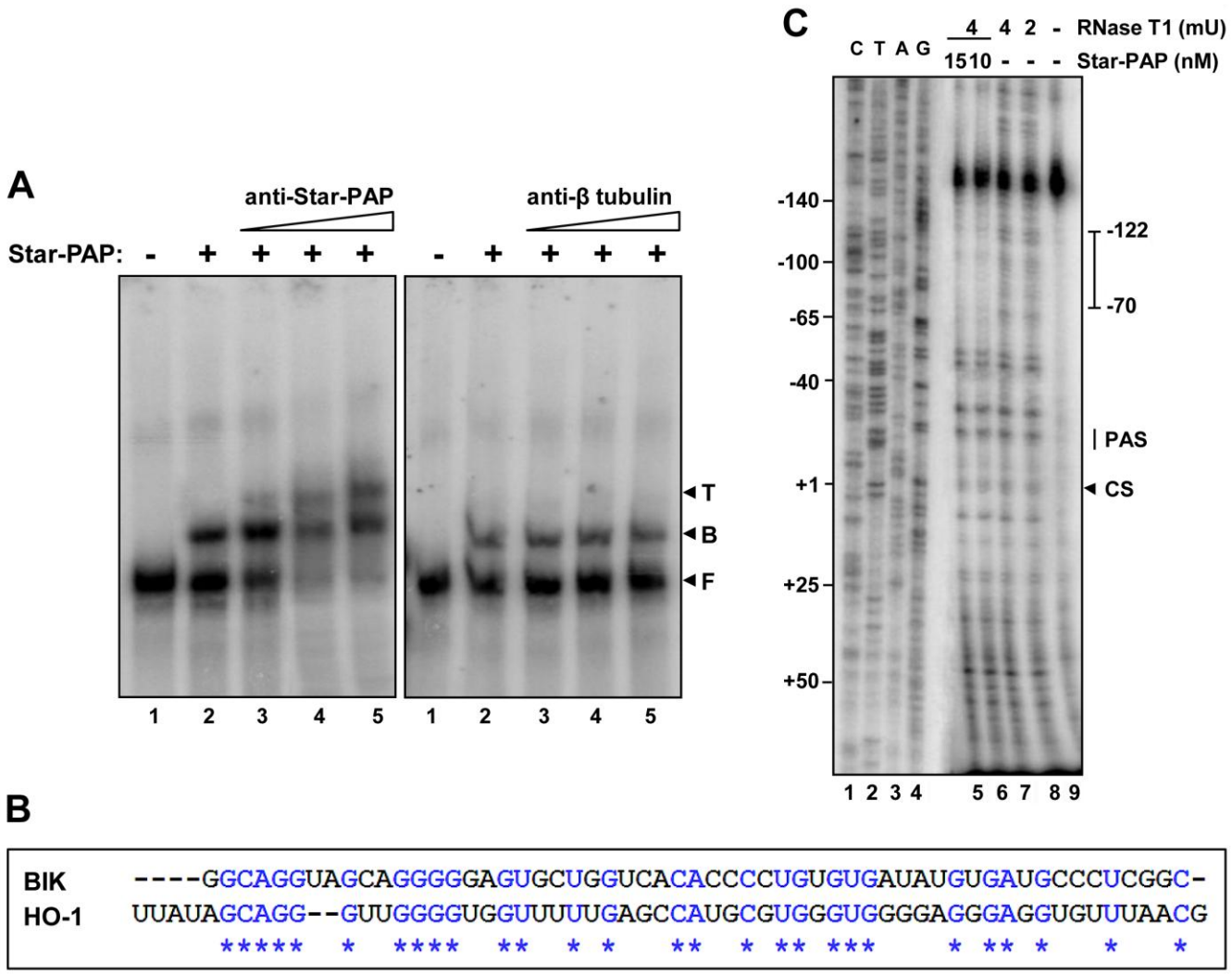

Figure S6. Analysis of Star-PAP Binding to BIK 3'-UTR and Comparison of the Binding Regions in *BIK* and *HO*-1 UTR RNAs

(A) EMSA of *BIK* UTR RNA with 15 nM Star-PAP in presence of increasing Star-PAP antibody (antibody super shift) (left panel) or β-tubulin antibody (right panel). Unbound RNA (F), Star-PAP-BIK RNA binary complex (B) and antibody, Star-PAP and RNA ternary complexes (T) are indicated.

(B) Sequence alignment of the Star-PAP binding regions on the *BIK* and *HO-1* UTR RNAs. * indicates fully conserved residues highlighted in blue.

(C) Footprint of Star-PAP on *BIK* UTR RNA by RNase T1 probing. The digestion pattern with different RNase T1 concentrations (mU) in absence of Star-PAP (lane 7-8), or in presence of 10 nM or 15 nM of Star-PAP (lane 5-6), and the untreated *BIK* RNA (lane 9) are indicated. Sequencing ladder is shown in lane 1-4. Numbers refer to the position of nucleotides with respect to cleavage site (CS). PAS = poly(A) signal. See also Figure 6.

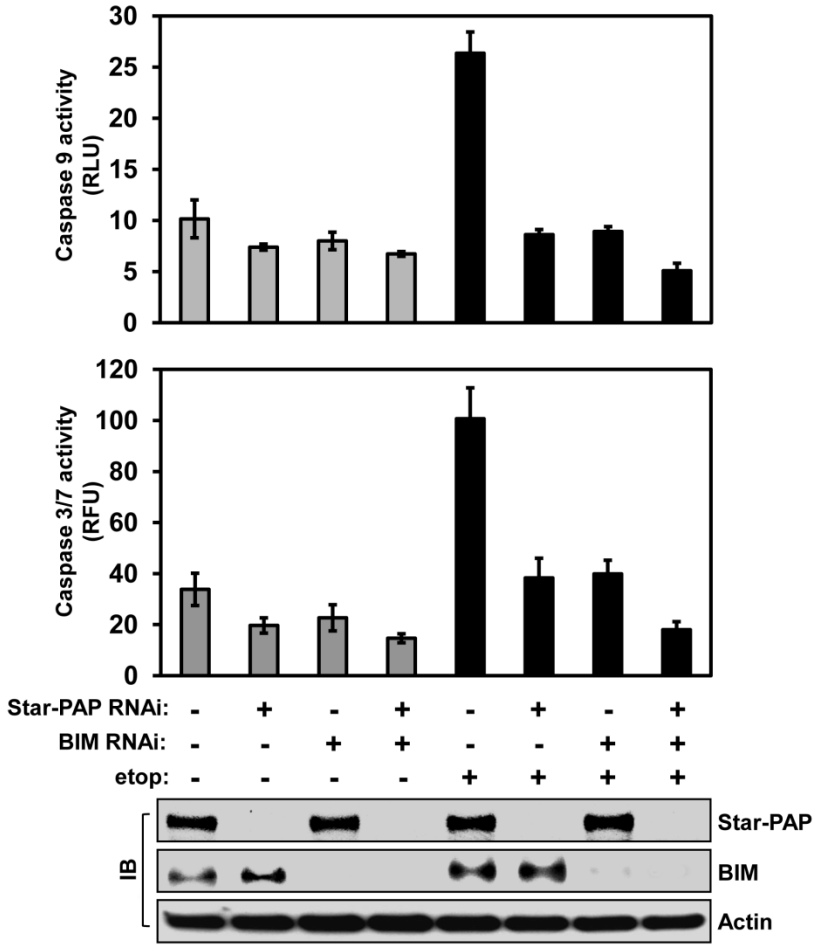

Figure S7. Star-PAP and BIM Knockdown Prevented Etoposide-Induced Apoptosis

Caspase 9 and caspase 3/7 activities were measured to evaluate the degree of apoptosis. The efficiency of Star-PAP and BIM knockdown was illustrated by IB at the bottom panels. Error bars represent standard error of the mean (SEM) of 3 independent experiments with triplicate for each experimental condition. See also Figure 7.

Supplemental Experimental Procedures

Plasmids and Constructs

The wild type and the polymerase-dead (D216/218A) Star-PAP as well as the wild type and the kinase dead (D322A) PIPKIα mutant cDNAs were inserted into the pCMV-Tag4a (Stratagene) vector through EcoRI and SalI restriction sites. PKCδ wild type and kinase-dead plasmids were purchased from "Addgene (#16386, 16389)". Silence-resistant mutations were generated in the Star-PAP, PIPKIα, and PKCδ cDNAs to render it insensitive to the siRNA oligos.

Protein Kinase Assay

The kinase assay was carried out in 1X kinase buffer containing 4 mM MOPS pH 7.2, 5 mM $MgCl_2$, 3 mM $MnCl_2$, 1 μM ATP, 0.5 mM DTT, 5 μM sodium orthovanadate, supplemented with 2 μg of MBP or affinity purified Star-PAP, PMA, $PI4,5P_2$ micelles in NP-40 (0.04%, final). The assay was initiated by adding [γ-^{32}P]ATP to the mixture and further incubated at room temperature (20 – 25 °C) for 30 min. The reaction was stopped by adding sample buffer to the mix and heated at 95 °C for 5 min. The samples were then subjected to SDS-PAGE followed by phosphorimaging with a Storm 840 phosphorimager (Molecular Dynamics) and quantified using the ImageQuant 5.1 software (Molecular Dynamics). Quantification of the kinase activities was normalized to the substrate-only lane.

RNase Footprinting

The RNA Footprinting was carried out by probing the *BIK* UTR RNA fragment with RNase S or RNase T1 followed by the detection of the cleaved fragments by extension of a primer complementary to the 3'-end of *BIK* RNA as described (Damgaard et al.,

1998; Murakawa and Nierlich, 1989). Around 0.5 nM of RNA was incubated in 20 μl of EMSA buffer in presence or absence of 0 - 15 nM of Star-PAP followed by digestions with indicated amounts of either RNase S or RNase T1 (2 – 4 mU) at RT for 15 min and primer extension after the enzymatic cleavage as described (Laishram and Anderson, 2010). A marker sequence was generated by dideoxy sequencing (Sequenase Quick-Denature sequencing Kit, USB Corps) from the template DNA of *BIK* UTR RNA with the same primer used for extension.

Detection of Caspase Activities

After RNAi knockdown, 10^4 cells/well were reseeded in 96-well plates and let grow for 24 h followed by etoposide treatment. Caspase 9 (after 4 h, Caspase-Glo9 Assay kit, Promega #G8210) and Caspase 3/7 activities (after 24 h, Apo-ONE Homogeneous Assay kit, Promega, #G7792) were measured using BioTek Synergy 2 microplate reader (BellBrook Labs) according to the manufacturers' instructions. Triplicate wells for each experimental condition were used.

SiRNAs Used in the Experiments

scrambled non-targeting: AGGUAGUGUAAUCGCCUUG

Star-PAP: GUGUGUUUGUCAGUGGCUU

PIPKIα: GAAGUUGGAGCACUCUUGG

PKCδ: AACCAUGAGUUUAUCGCCACC

BIM: CAGAGAUAUGGAUCGCCCAAGAGUU

Primers Used for Gene Expression

BIK forward: 5'-TCTTGATGGAGACCCTCCTG-3'

BIK reverse: 5’-GTCCTCCATAGGGTCCAGGT-3’

GAPDH forward: 5’-GAAGGTCGGAGTCAACGGATTT-3’

GAPDH reverse 5’-GAATTTGCCATGGGTGGAAT-3’

Primers Used for RIP

BIK forward: 5’-GTCACACCCCTGTGTGATATGTGATGC-3’

BIK reverse: 5’-GCAGGGAAGGATCTGATTAGGAGCACACAG-3’

GCLC forward: 5′-GATGATTAAAGAATGCCTGGTT-3′

GCLC reverse: 5′-TATGCTTCTTTCTAGAAACATC-3′

Primers Used for mRNA 3’-End Cleavage

BIK forward: 5’-GTCACACCCCTGTGTGATATGTGATGC-3’

BIK reverse: 5’-GCGAGAGGAAGCCCGTGCTGGTGCTGCC-3’

Primers Used for mRNA 3’-RACE

BIK: 5’-GGCCTGCTGCTGTTATCTTT-3’

GAPDH: 5’-GTATGACAACGAATTTGGCTACAGCAAC-3’

Primer Used for Extension and Sequencing in RNA Footprinting

5’- TGCGGTCCCCTTTTGCAGGGA -3’.

Antibodies Used

Rabbit polyclonal anti-Star-PAP and anti-PIPKIα (Anderson’s Lab homemade) (Mellman et al., 2008); rabbit polyclonal anti-PKCδ (Santa Cruz Biotechnology, #sc-937); mouse monoclonal anti-PKCδ (Zymed, #41-0300); mouse monoclonal anti-SC35 (BD-Pharmingen, #556363); mouse monoclonal anti-Flag (Sigmal Aldrich, #F1804); goat

polyclonal anti-BIK (Santa Cruz Biotechnology, #sc-1710); rabbit polyclonal anti-BIM (Santa Cruz Biotechnology, #sc-11425); mouse monoclonal anti-RNA Pol II (neoclone, #WP011); rabbit polyclonal anti-BAX (Santa Cruz Biotechnology, #sc-493); mouse monoclonal anti-T7.Tag (Novagen, #69048); mouse monoclonal anti-HA (Covance, #MMS-101P); mouse monoclonal anti-β-tubulin (Upstate Biotechnology, #05-661); mouse monoclonal anti-actin (MP Biomedical, #691002).

Supplemental References

Damgaard, C. K., Dyhr-Mikkelsen, H., and Kjems, J. (1998). Mapping the RNA binding sites for human immunodeficiency virus type-1 gag and NC proteins within the complete HIV-1 and -2 untranslated leader regions. Nucleic Acids Res *26*, 3667-3676.

Murakawa, G. J., and Nierlich, D. P. (1989). Mapping the lacZ ribosome binding site by RNA footprinting. Biochemistry *28*, 8067-8072.